Cairo University
Faculty of Engineering
Aeronautical and Aerospace Department

CU-M.A.V. VER 1.0

Submitted For B.Sc. Graduation Project

Submitted by:

Abd El Rahman El-Saied   Akram Mahmoud   Tarek M. El Banna

I   Abstract

This project is a first step investigation into micro air vehicles. Micro air vehicles are very small flying surveillance unmanned air systems, able to follow a preset path or be remotely controlled. The designated mission would be short range surveillance, status monitoring, and hazardous sensor deployment. This paper handles the design and construction of such aircraft from the perspective of achieving the maximum possible flight duration. A number of research papers discussing aerodynamics at low speeds were referred to as a launch platform for the design process. Further analysis was performed computationally to produce more specific data. Empirical study of said data was afterwards carried out to test design stability. A number of prototypes were built and tested, both statically and dynamically. The results showed that production of such a small scaled vehicle was both possible and feasible. In addition to that conclusion, it was apparent that more research would be needed to fully and effectively realize the potential of micro air vehicles. The following phases will include adding an autopilot subsystem, micro camera and transmitter and maximizing payload to allow for more sophisticated sensing apparatus to be deployed.

II Contents

P r e f a c e

III Table of figures

IV Acknowledgements

1   CHAPTER ONE: OVERVIEW

1.1   Introduction:

Everything in our world is tending to be more versatile, compatible, smaller, reliable, and economical. The Micro Air vehicle (MAV) is a venture in that direction. This concept was initiated in the United States military in 1993 by Hindley and Richard and the concept of an insect based crawling system developed. Later, between 1993 and 1995, feasibility studies were conducted and the results were affirmative. (See fig. 1.1)

There is a serious effort till now days to design an aircraft that is as small as possible for special, limited-duration military and civilian missions. These very small airplanes did not have an appropriate definition till DARPA (Defense Advanced Research Project Agency) defined them as micro air vehicles (MAVs), and they are of interest because electronic surveillance and detection sensor equipment can now be miniaturized so that the entire payload mass is less than 18 g. Now days the main goal is develop an aircraft with a 15-cm maximum dimension that have a mass of less than 100 g.
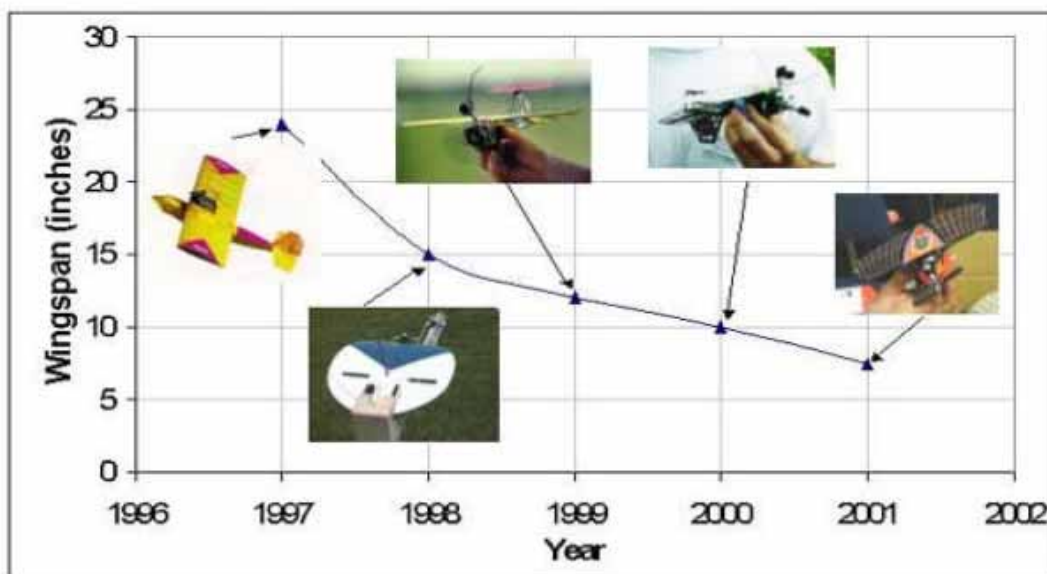
Figure 1.1

1.2   Challenges

In 1997, the United States Defense Advanced Research Projects Agency (DARPA) launched an initiative to develop MAVs for the battlefield arena. This initiative prompted the design and development of a number of flying vehicles including the six-inch wingspan Black Widow by Aerovironment, the MicroStar

Overview

project by Lockheed Sanders, and the MITE prototype vehicle by Naval Research Laboratories.

There are a number of formidable challenges to designing aircraft at the MAV scale that are not present when designing larger scale vehicles. These challenges fall into three broad categories:

1. Aerodynamic efficiency,

2. increased wing loading

3. Stability and control.

As vehicle size decreases, the viscous effects of the airflow, which are generally ignored in the design of large-scale aircraft, begin to have a significant impact on aerodynamic performance. On the MAV scale, the laminar flow that prevails is easily separated, creating large separation bubbles, especially at higher angles of attack. Even the best airfoils on the MAV scale have lift to drag ratios almost an order of magnitude smaller than their larger scale counterparts.

The challenges related to wing loading are a direct result of the scale of these aircraft. As the wingspan of flying vehicles decreases, the mass of the required structures for the vehicle increase relative to the wing area. Biological studies have shown that wing loading of birds and insects increases linearly with a reduction wing area due to the fundamental material properties of their structures. This feature of scaling down requires all subsystems of MAVs to be as lightweight as possible.

Stability and control presents perhaps the most difficult challenge in deploying operational and usable MAVs. The low moments of inertia of MAVs make them vulnerable to rapid angular accelerations; a problem further complicated by the fact that aerodynamic damping of angular rates decreases with a reduction in wingspan. Another potential source of instability for MAVs is the relative magnitudes of wind gusts, which are much higher at the MAV scale than for larger aircraft.

In fact, wind gusts can typically be equal to or greater than the forward airspeed of the MAV itself. Thus, an average wind gust can immediately affect a dramatic change in the flight path of these vehicles. From our own early flight tests, it has become clear that a very robust control system is indeed required for practical flight missions on the MAV scale.

The design of an effective MAV control system is further complicated by the limits of current sensor technology. The technologies used in rate and acceleration sensors on larger aircraft are not currently available at the MAV scale. It has proven very difficult, if not impossible, to scale these technologies down to meet the very low payload requirements of MAVs. While a number of sensor technologies do currently exist in small enough packages to be used in MAV systems, there is a tradeoff between accuracy and size. Take, for example, MEMS (Micro Electro-Mechanical Systems) rate gyros and accelerometers. MEMS piezoelectric gyros, while only weighing approximately one gram, have drift rates on the order of per minute and are highly sensitive to changes in temperature. While elaborate temperature calibration procedures can improve their accuracy to some degree, their use in inertial navigation is difficult at best. So in addition of being a compact system transportable by a single operator, MAVs have other advantages.

Overview

1.3 Advantages of MAVs

Cost efficiency and the versatility of MAVs caught major attention of military applications. MAVs are a subset of UAVs characterized by their relatively small size. This small size implies a number of potentialities to include the following:

4. MAVs may prove a cost-effective augmentation to existing, overtaxed systems

5. real time surveillance

6. battlefield damage assessment

7. can perform search and rescue operations

8. monitoring concentrations of chemicals in agricultural or industrial spills

9. traffic monitoring

10. hostage crisis monitoring

11. locating illegal drugs or weapons

12. MAVs may afford a commodity approach to mission accomplishment either by enabling a variety of payloads to be manufactured for a single airframe or by proving flexible enough to permit payload variation in the field

13. MAVs may bring mission capabilities to smaller units that heretofore were not large enough to justify possession and operation of traditional systems providing such capabilities.

14. MAVs may be more amenable to a faster, better, cheaper approach to their development, procurement, and fielding. It should be possible to design MAVs to have a small (even negligible) logistics footprint.

15. rapid development

16. Real-time data acquisition capability

17. low radar cross section

18. The potential for low production cost

19. low noise
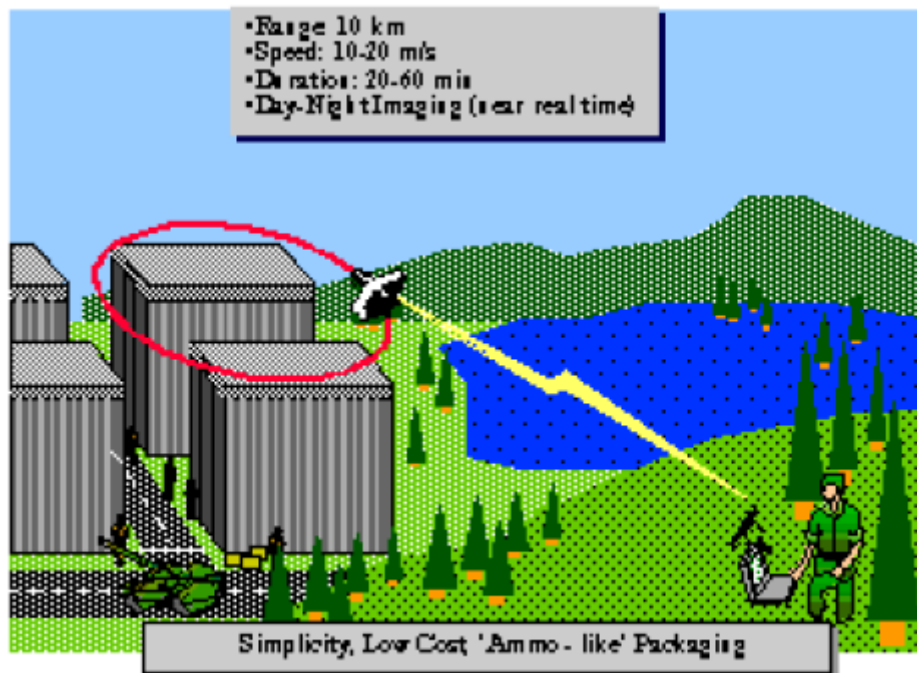
Figure 1.2-a **The "Over-The-Hill Reconnaissance" Mission for the MAV**
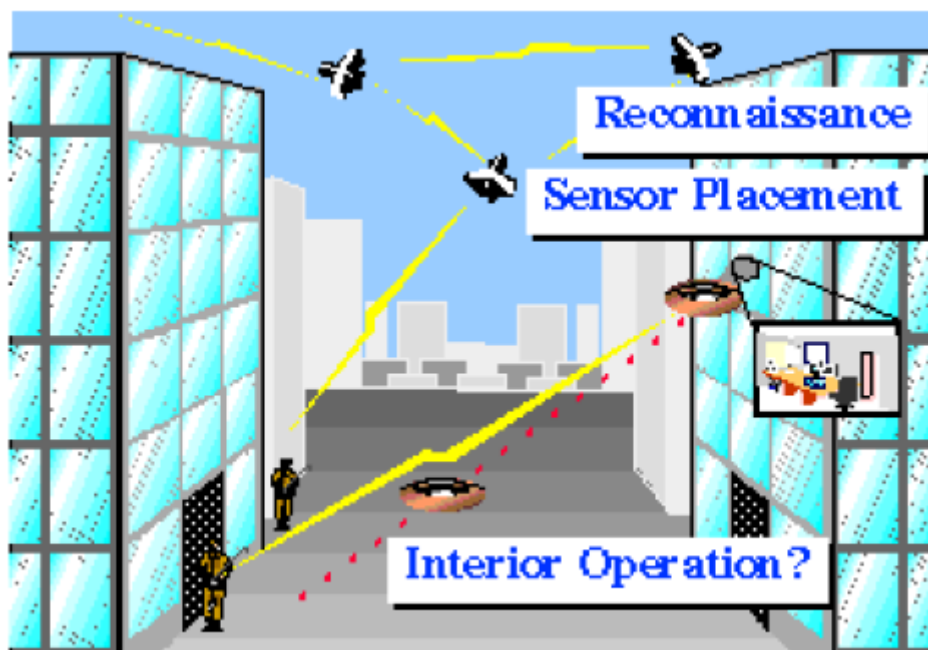
Figure 1.2-b **Urban Operations Missions for the MAV**
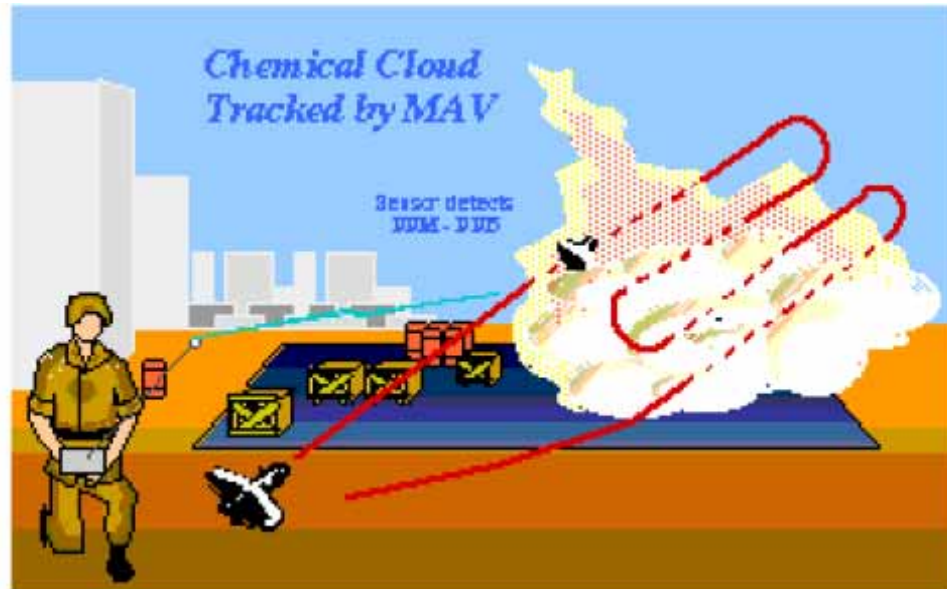
Figure 1.2-c **The MAV as a Mobile Immersion Sensor**

The primary missions of interest for fixed wing MAVs include surveillance, detection, communications, and the placement of unattended sensors. Surveillance missions include video (day and night), infrared images of battlefields (referred to as "around the corner"). These real-time images can give the number and the location of opposite forces. This type of information can also be useful in hostage rescue and counter-drug operations. Because of the availability of very small sensors, detection missions include the sensing of biological agents, chemical compounds, and nuclear materials (i.e., radioactivity). MAVs may also be used to improve communications in urban or other environments where full-time line-of-sight operations are important. The placement of acoustic sensors on the outside of a building during a hostage rescue or counter-drug operation is another possible mission.

The requirements for a fixed wing MAVs include a wide range of possible operational environments, such as urban, jungle, maritime, and mountains. Furthermore, MAVs must be able to perform their missions in all weather conditions (i.e., precipitation, wind shear, and gust). Because these vehicles fly at relatively low altitudes (i.e., less than 100m) where buildings, tree, hills, etc. may be present, a collision avoidance system is also required.
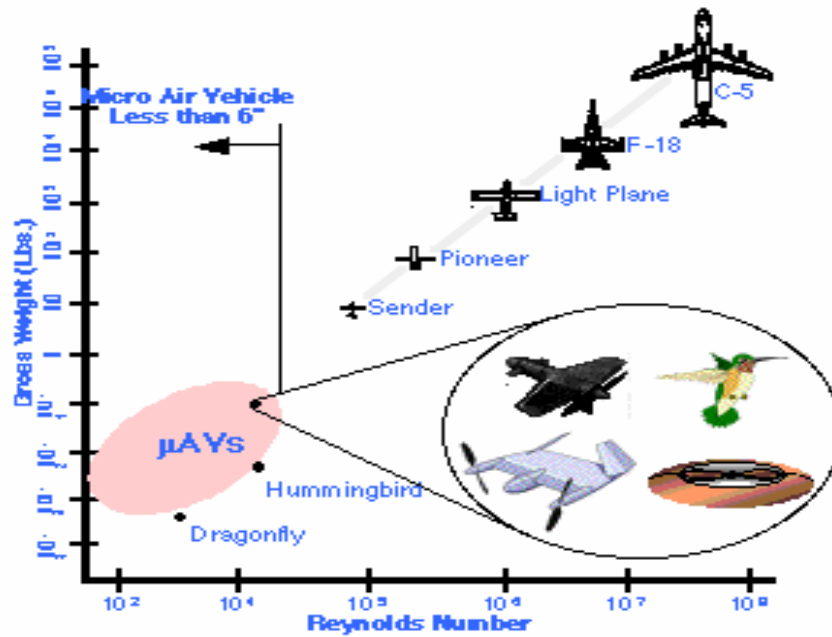
Figure 1.3   **Comparison of MAVS' flight regime with others**

Significant technical barriers must be overcome before MAV systems can be realized. These include issues in small-scale power generation and storage, navigation, and communications as well as propulsion, aerodynamics, and control. One of the most interesting and least understood aspects of small-scale flight is the aerodynamics. The combination of small length scale and low velocities results in flight regime with Reynolds numbers. This places MAVs in a regime totally alien to conventional aircraft. The gross mass of MAVs and other flying objects vs. Reynolds number is shown in fig. 3. The payload mass vs. wingspan for MAVs and unmanned air vehicles (UAVs) is presented in fig. 4.

16

Overview
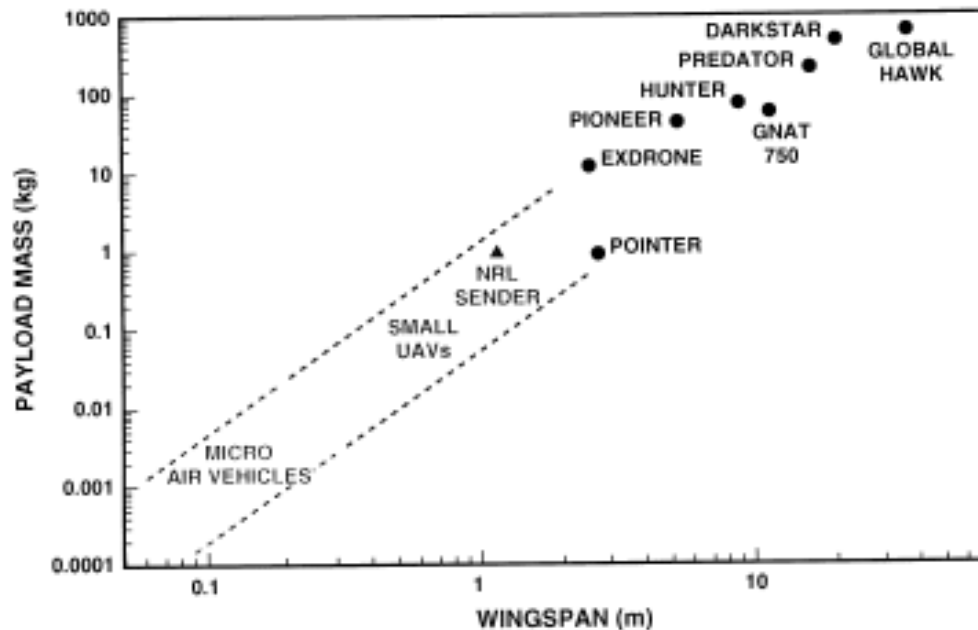
Figure 1.4 payload mass vs. wingspan

The long term goal is to develop aircraft systems with a mass of less than 30 g, a wingspan of about 8 cm, and an endurance of 20 to 30 min at speeds between 30 to 65 km/h. It appears that flapping or rotary wing designs may have advantages over a fixed wing MAVs at this small size. One of these advantages is in the generation of the lift and thrust without excessive size or weight. The interest in achieving insect like or birdlike flight performance has focused attention on their wing dynamics and unsteady aerodynamics. However, our understanding of aerodynamics of bird and insect flight is limited. Biologists have studied bird and insect flight empirically for a quite some time. One thing that is clear from these investigations is that all of these creatures use two specific mechanisms to overcome the small-scale aerodynamic limitations of their wings: flexibility and flapping. Birds and insects exploit the coupling between flexible wings and aerodynamic forces (i.e., aero elasticity) such that the aero elastic wing deformations improve aerodynamic performance. By flapping their wings, birds and insects effectively increase the Reynolds number seen by the wings without increasing their forward flight speed. Although some progress has been made in mimicking avian aeromechanics, more is necessary if an operational flapping wing MAV is to be successful.

17

Overview

We will talk now more about the fixed wing vehicles:

The design requirements cover a wide of parameters for micro air vehicles. The MAV must be designed as a system consisting of airframe, propulsion, payload, and avionics. Although much smaller than operational fixed wind UAVs, electrically powered MAVs will have approximately the same weight fractions, that is 12% for the airframe, 11% for the engine, 30% for the battery, 21% for the payload, and 17%for the avionics and miscellaneous items *(private communication with R. J. Foch, Naval Research Laboratory, Washington DC, 1996)*. Minimum wing area of ease of packaging and pre-launch handling is also important.

The airfoil section and wing plan-form of the lifting surface occupy a central position in all design procedures for flying vehicles. Also, as with all aircraft, MAVs share the ultimate goal of stable and controllable vehicle with maximum aerodynamic efficiency. Aerodynamic efficiency is defined in terms of lift-to-drag ration. Airfoil section $C_{l_{max}}$, $C_{d_{max}}$, and $(C_l/C_d)_{max}$ as function of Reynolds number are shown in figs. 5a, 5b, and 5c for two-dimensional airfoils (i.e., infinite wings). It is clear from the figure (adapted from Ref. McMasters, j. H., and Henderson, M. L., "Low Speed
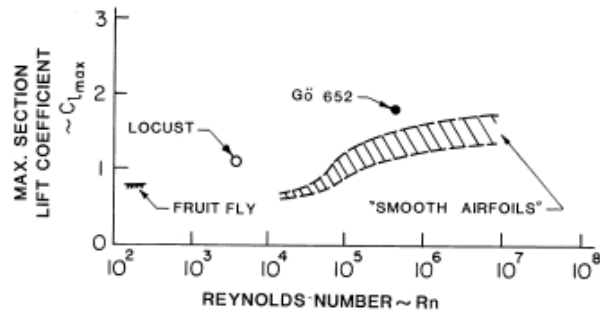
(a) Maximum lift coefficient
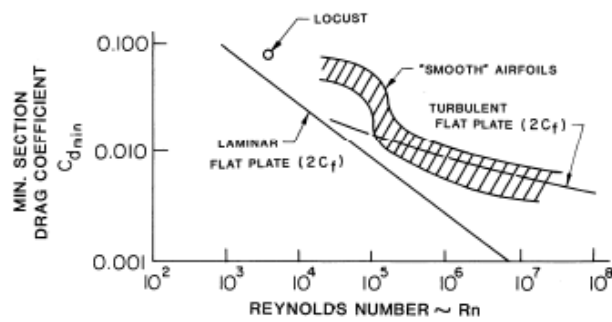
(b) Minimum drag coefficient
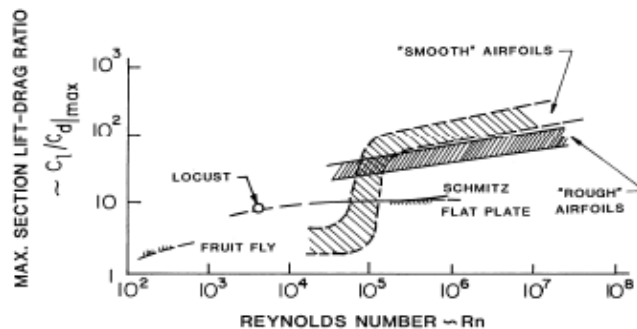
(c) Maximum lift-to-drag ratio

Figure 1.5   Airfoil Performance

O v e r v i e w

Single Element Airfoil Synthesis," Technical Soaring, Vol. 2. No.2, 1980, pp.1-21) that the airfoil performance deteriorates rapidly as the chord Reynolds number decreases below 100,000. Performance of three-dimensional wings (i.e., finite wing), as measured by $(Cl/Cd)_{max}$, is less than that for airfoils except when wing aspect ration is reduced below a value of 2. While the maximum lift-to-drag ration for most low speed fixed wing aircraft including UAVs ($U\infty < 5o$ m/s) is greater than 10, values for insects and small birds are usually less than 10. Furthermore, to achieve these values for MAVs at Reynolds numbers, the wings must emulate bird and insect airfoils and be very thin (i.e., t/c < 0.06) with a modest amount of chamber.

Requirements for typical propellers-driven fixed wing MAVs, for example, include long flight duration (i.e., high value of $Cl^{3/2}/Cd$ at speeds up to 65 km/h at chord Reynolds numbers from about 45,000 to 180,000 and altitude from 30 to 100 m). Because these vehicles are essentially small flying wings, there is a to develop efficient low Reynolds number, low aspect ratio wings that are not overly sensitive to wing shear, gust, and the roughness produced by precipitation. Furthermore, confidence that the operational vehicle will perform as designed is important in all applications.

Although design methods developed over the past 35 years produce efficient airfoils for chord Reynolds numbers greater than about 200,000, these methods are generally inadequate for chord Reynolds numbers below 200,000, especially for very thin airfoil sections. In relation to the airfoil boundary layer, important areas of concern are the separated regions that occur near the leading and/or trailing edges and transition from laminar to turbulent flow if it occurs. It is well known the separation and transition are highly sensitive to Reynolds number, pressure gradient, and the disturbance environment. Transition and separation play a critical role in determining the development of the boundary layer, which affects the overall performance of the airfoil/wing. The aerodynamic characteristics of the wing and other components, in turn, affect the static, dynamic, and aero elastic stability of the entire vehicle. Therefore the successful management of the sensitive boundary layer for particular low Reynolds number vehicle designs in critical.

Laminar separation bubbles occur on the upper surface of most airfoils at chord Reynolds numbers above about 50,000. In principle, laminar separation bubble and transition can be artificially controlled by adding the proper type of disturbance at the proper location on the airfoil. Wires, tape strips, grooves, steps, grit, or bleed-through holes in the airfoil have all been used to have a positive influence on the boundary layer in this critical Reynolds number region. The type and location of these are called turbulators. In fact, how the disturbance produced by the given type of turbulator influence transition is not completely understood.

$$CL_{AR=1} = a_{AR=1} + b_{AR=1}\,\alpha + c_{AR=1}\,\alpha^2$$

$$CL_{AR=x} = a_{AR=x} + b_{AR=x}\,\alpha + c_{AR=x}\,\alpha^2$$

$$CL_{AR=2} = a_{AR=2} + b_{AR=2}\,\alpha + c_{AR=2}\,\alpha^2$$

Rectangular Planform
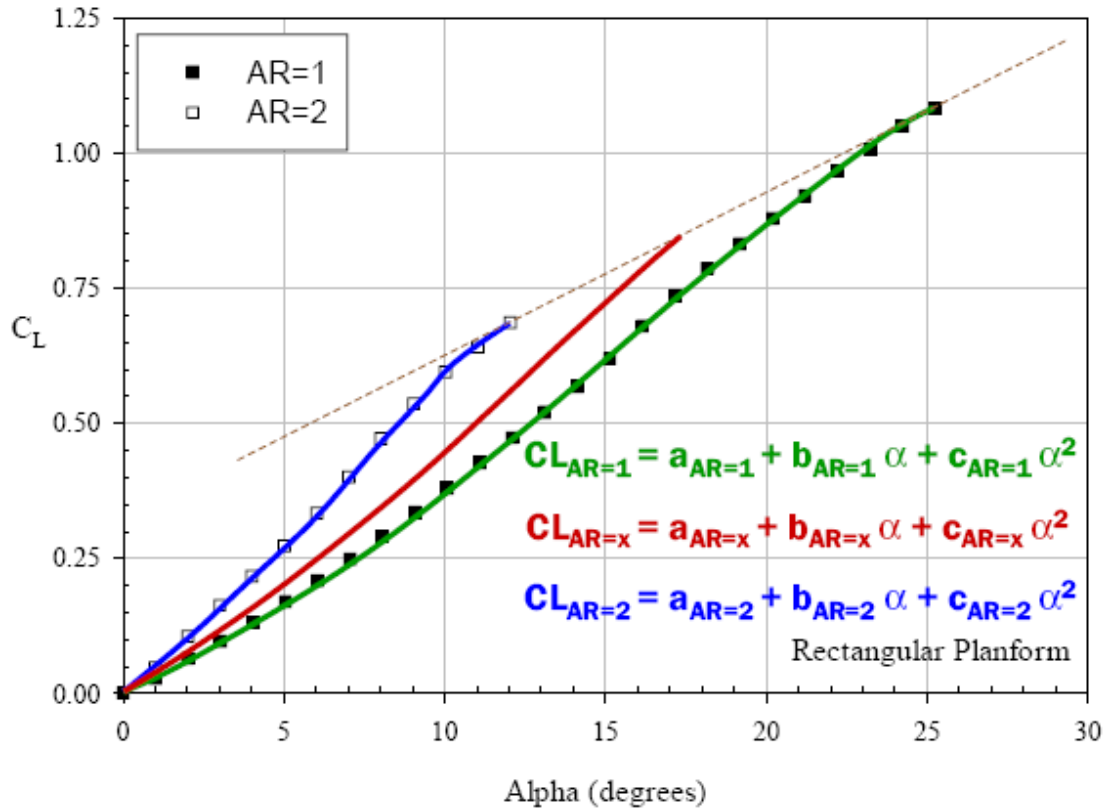
Figure 1.6   **Variation of C_l with Angle of attack Alpha**

The discussion of airfoils operating at low Reynolds number s presented above in based on a large number of experimental and analytical studies performed over the past decades. This understanding of airfoil performance have been very useful in the design of small UAVs with wingspans from 50 cm to 1 m (i.e., from about 200g to 4 kg total mass) and chord Reynolds number well above 200,000. These UAVs have wings of a large aspect ratio and thickness, which is characteristic of numerous successful vehicles. Recently, it has been found that for vehicles with aspect ratios around 1 and below 4, thin wings cannot be designed using existing airfoil data. For these low aspect ratio wings (our case), the larger component of lift is produced by the tip vortices, which influence the majority of the wing surface. For example, at a chord Reynolds number of 100,000, the lift coefficient for an elliptical plan form flat-plat wing with AR = 2 reaches its maximum value at an angle of attack of about 12 deg. As seen in fig. 6, at the same Reynolds number for AR = 1 elliptical plan form flat-plate wing, the lift coefficient continues to increase past 25 deg. This behavior is similar in delta wing.

1.4   Concluding remarks:

We are focused on the understanding of aerodynamics issues related to micro air vehicles design and performance.

Overview

There are a lot of other questions have been surfaced from studies like, for example, whether camber is really beneficial at low Reynolds numbers and whether an optimum combination of plan form shape and camber exists for maximized performance and stability. Other question include location and size of control surfaces, the influence of propeller flow field on the lift and drag of MAVs, and feasibility of designing wing tips that can control the low-frequency rolling characteristic of low aspect ratio wings.

We will try to answer these questions by further CFD solution simulation and flight tests.

2 CHAPTER THREE: AERODYNAMIC CHARACTERISTICS OF LOW ASPECT RATIO (LAR) WINGS AT LOW R$_e$

2.1 Introduction

One of the most important aspects considering a design of an air vehicle is the aerodynamics study. However when concerned with Micro Air Vehicle aerodynamics study becomes a serious challenge. This is because of the low aspect ratio (LAR) a MAV fly within. This regime of flight is a new born aerodynamics study field.

To design this project's MAV a detailed study of a paper prepared by *Gabriel E. Torres, "Aerodynamics of Low Aspect Ratio Wings at Low Reynolds Numbers with Applications to Micro Air Vehicle Design"*, was carried out. This chapter presents the study for this paper, as well as a number of other researches, as a stepping stone for designing the MAV. That's to say, selection of airfoils, plan-form and aspect ratio.

2.1.1 MAV Definition:

- Max Dimension= 15 cm

- Operation rang= 10 Km

- Pay load = Up to 18 g

- R_e =50,000 to 250,000 (roughly)

- Low Aspect Ratio (AR) wings (LAW): About 1

- Average endurance = 30 min

- Cruising speeds = 15 to 80 km/Hr

2.1.2 Lift Sources in MAVs:

Studies were made on the low Aspect ratio affect on the flight in low R_e regime as interests about Micro Air Vehicles (MAVs) grew rapidly over the last period. Studies were made on different plan forms and found that delta wings plan forms are not ideal because for a given max dimension, delta wings offer less lifting area. Information regarding non-delta LAR wings is available since 1950 (made between 1930-1950). Zimmerman, Berlett and Vidal and Wadlin et al. performed experiments on LAR wings although at significantly greater R_e. Some other theoretical and analytical treatises of LAR wing aerodynamics have been made by Bolly, Weinig, Bera and Suresh, Polhamus, and Rajan and Shashidhar to name a few.

Probably the most complete analysis was made Hoerner in his two volume series on lift and drag. Hoerner information was built on higher R_e than that this study is interested in but still the aerodynamics theory holds.

This theory correctly predicts that as a finite wing of a given Aspect Ratio generates lift, counter-rotation vertical structures form near the wingtips. These vortices strengthen as the angle of attack increases. For out case (LAW wing) the tip vortices may be present over most of the area and therefore exert great effect on the aerodynamic characteristics. Wings of AR less than or equal to 1 can be consider to have to sources of lift; a. Linear and b. Non-Linear.

a) The linear lift is formed due to circulation around the airfoil typically to what is thought of lift generated in higher AR wings.

b) The Non linear lift is created due to formation of low pressure cells on the wing's top surface by tip vortices. This non-linear effect increases the lift-curve slope as the angle of attack increases and it is considered to be responsible for the high value of "stall angle of attack".
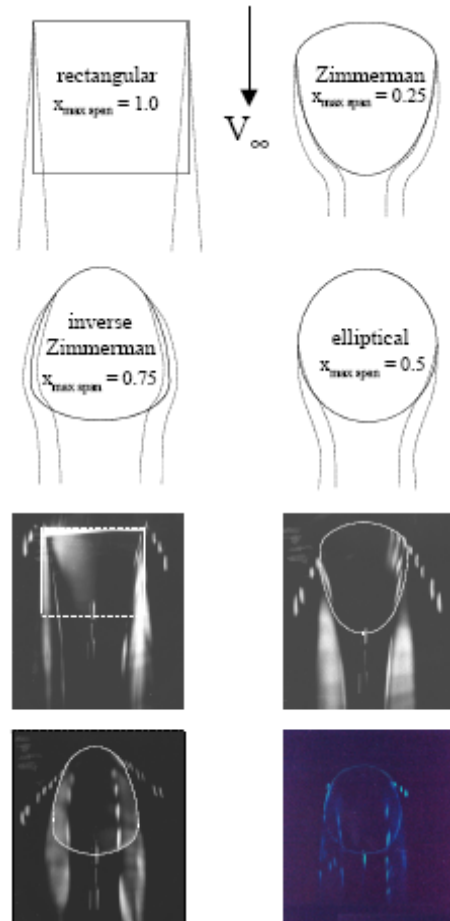
Figure 2.1 Schematic of wing vortices for each wing plan form shape
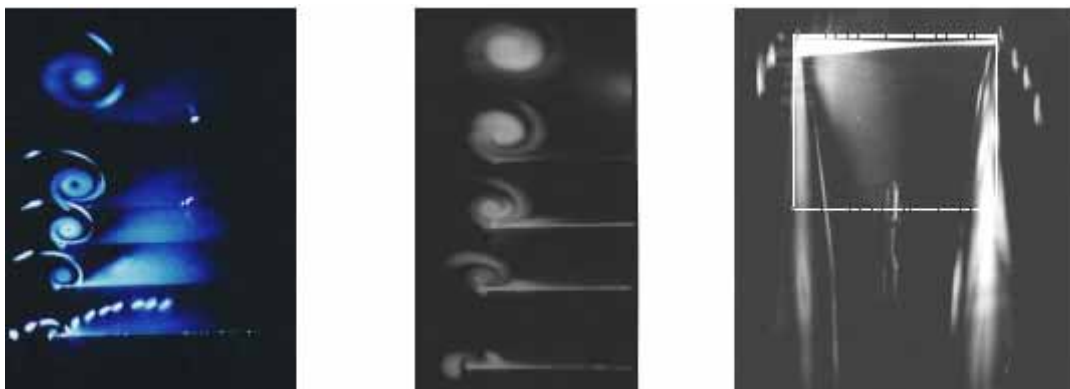
Figure 2.2 Wingtip Vortices, rect1.00 Wing, Re ≈70,000, α = 15◦
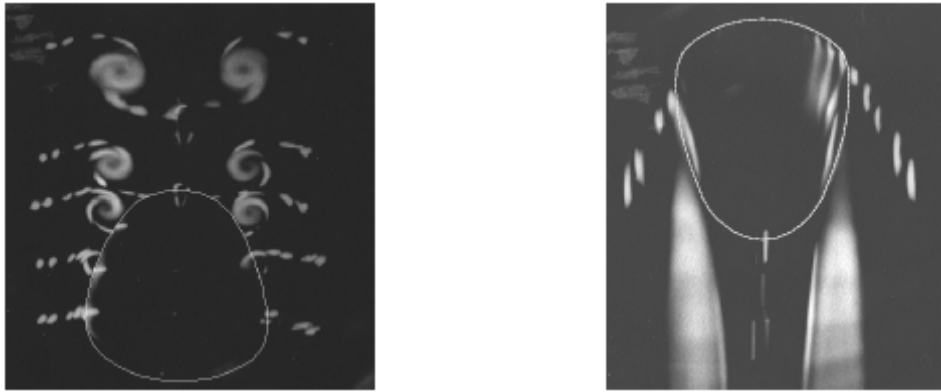
Figure 2.3 Wingtip Vortices, zim1.00 Wing, Re ≈70,000, α = 15◦

Figure 2.4 Wingtip Vortices, ziminv1.00 Wing, Re ≈70,000, α = 15◦

Surface-fluid visualization was performed for three AR = 1 wings and one AR = 0.5 wing at several angles of attack. All experiments were conducted at a Reynolds number of approximately 70,000. Figure 4 shows photographs of the rect0.50 wing at six angles of attack. It can be concluded from these photographs that there exists a separation bubble near the leading edge for α between 7◦ and 11◦. Evidence of the separation bubble is found in the region near the leading edge of the wing where fluid is seen to accumulate. The most likely interpretation of this phenomenon is that the fluid in this stagnant region is located within the recirculating region of air trapped inside a separation bubble.

Furthermore, it can be observed that this separation bubble is limited to the inboard section of the wing. It is proposed that this is because near the wingtips, the tip vortices energize the flow and limit the development of the separation bubble.

Figure 5 shows that the separation bubble forms in the rect1.00 model for alpha between 5◦ and 7◦, and to some extent exists at alpha = 9◦. The large portion of the wing area which is affected by the tip vortices is apparent from the photographs at alpha = 11◦ and 15◦. The streak lines in the photograph at alpha = 9◦ are caused by small sediments in the fluid used for flow visualization.

For the zim1.00 model, the sequence of photographs in Figure 2.3 shows evidence of a separation bubble being present for angles of attack greater than 5∘ but less than 11∘. The influence of the tip vortices is almost non-existent as the bubble seems to extend to the wingtip at all angles of attack.

Finally, the ziminv1.00 model photographs of Figure 2.4 provide an interesting view of the tip vortices joining to become one U-shaped vortex tube as the angle of attack increases above 11∘. The separation bubble that seems to be present at alpha = 9∘ appears to become part of the vortex structure at higher angles of attack.
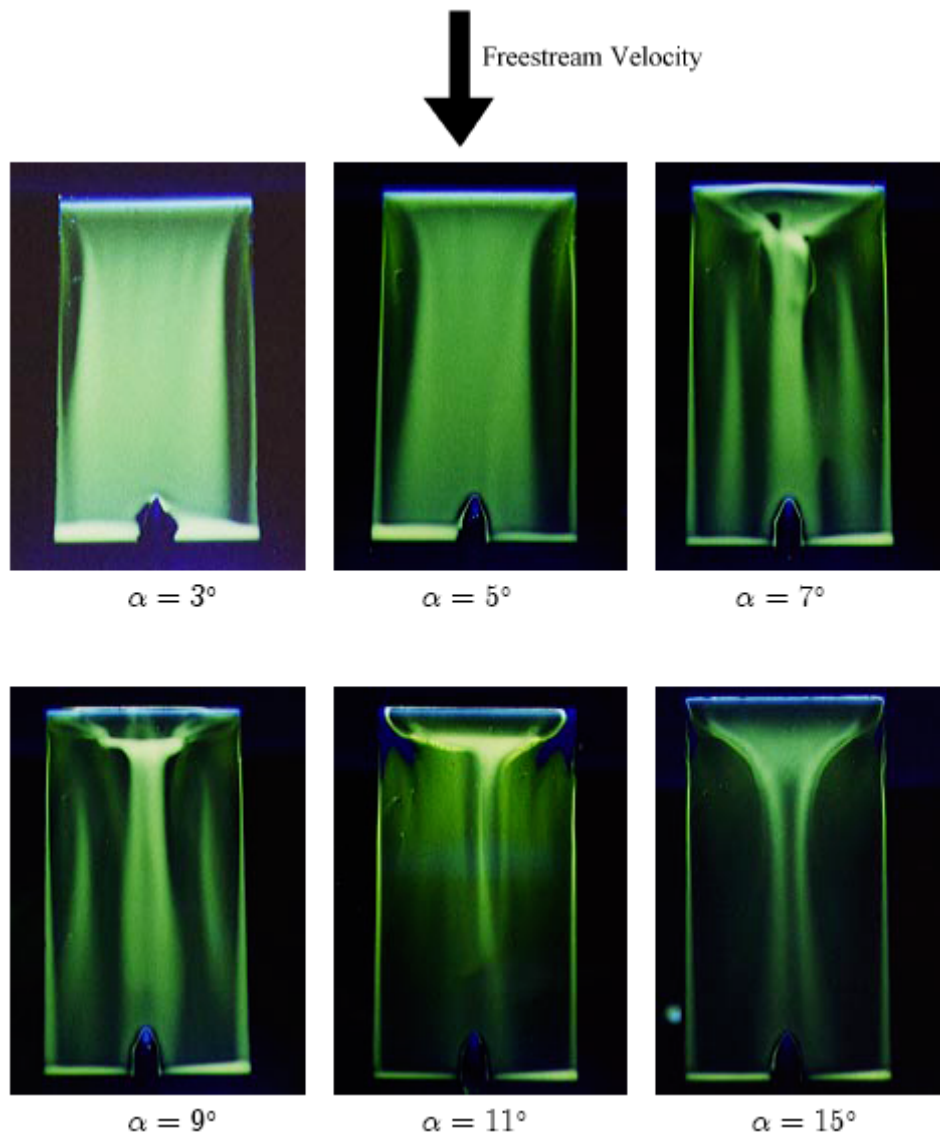
Figure 2.5 AR 0.5 Rectangular Wing Surface Visualization, Re = 70,000
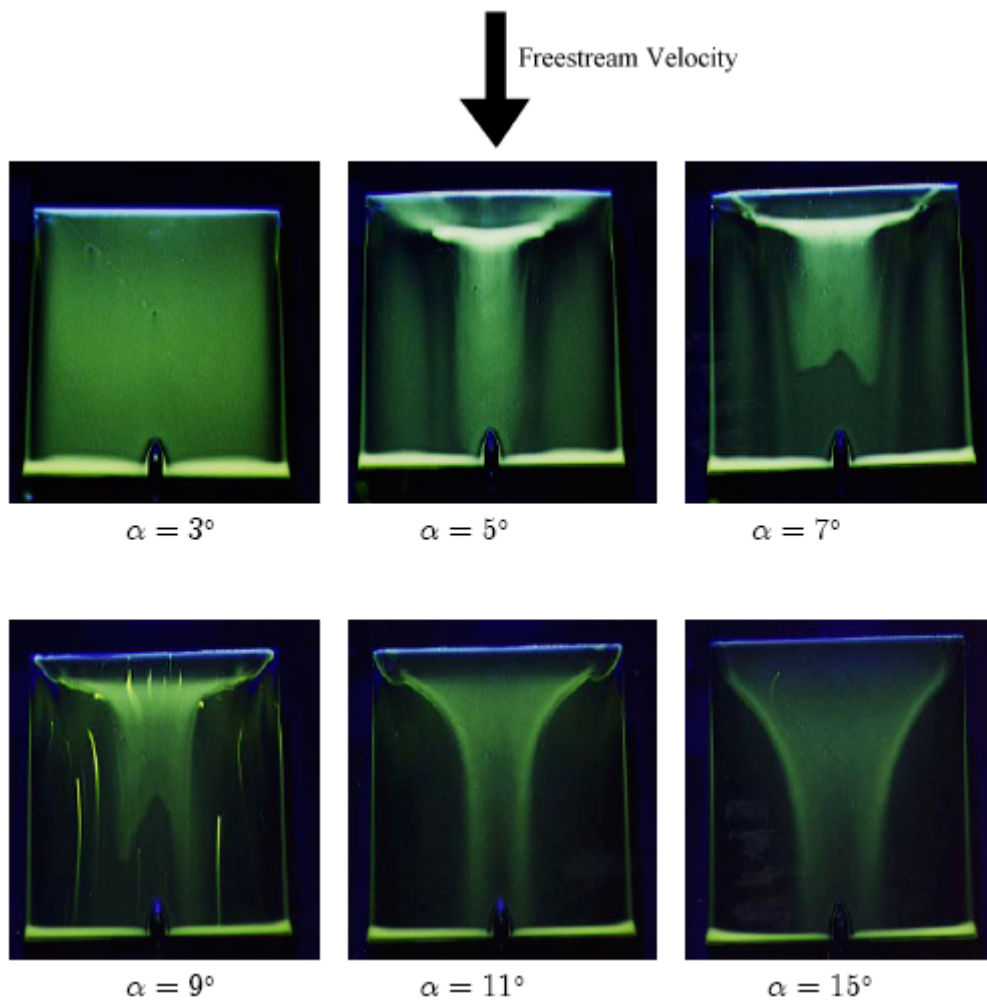
Figure 2.6 AR 1.0 Rectangular Wing Surface Visualization, Re = 70,000
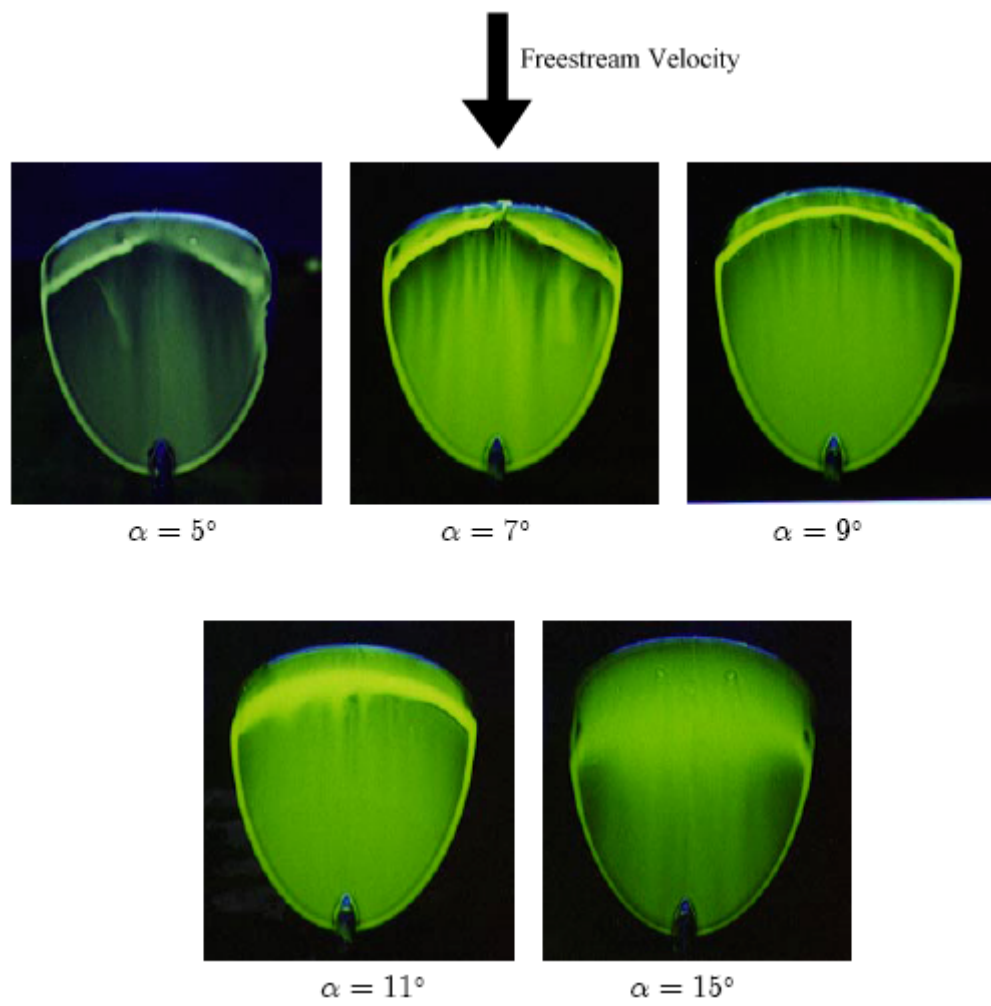
Figure 2.7 AR 1.0 Zimmerman Wing Surface Visualization, Re = 70,000
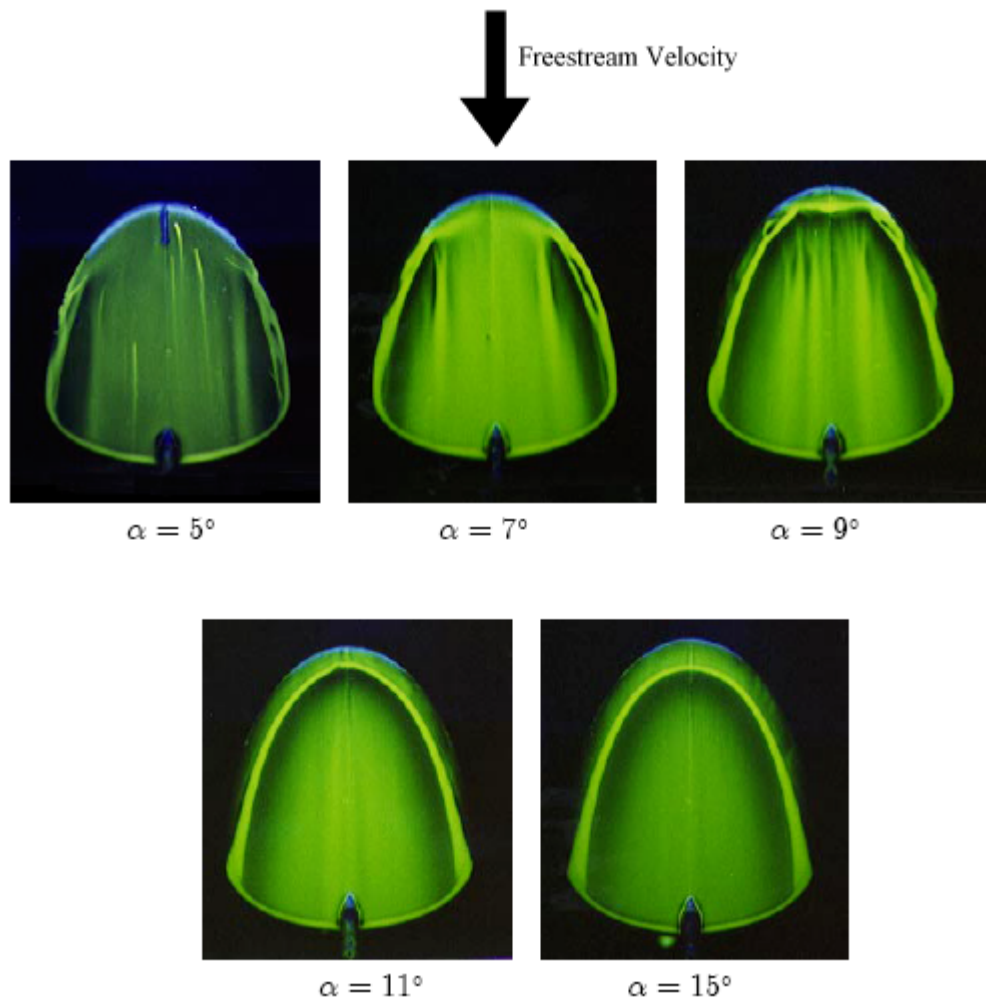
Figure 2.8 AR 1.0 Inverse Zimmerman Wing Surface Visualization, Re = 70,000

2.2 Wing Models

Several wings with different plan forms were tested by a study and all models had these specifications:

- Thickness to chord ratio of 1.96%.

- 5 to 1 Elliptical Leading edge / Trailing edge.

- Most models had root chord of 0.2023 m (20.32 cm).

- "Zimmerman" models were formed by joining 2 half-ellipses at either quarter-chord location (for Zimmerman) or at three-quarter location (inverse Zimmerman).
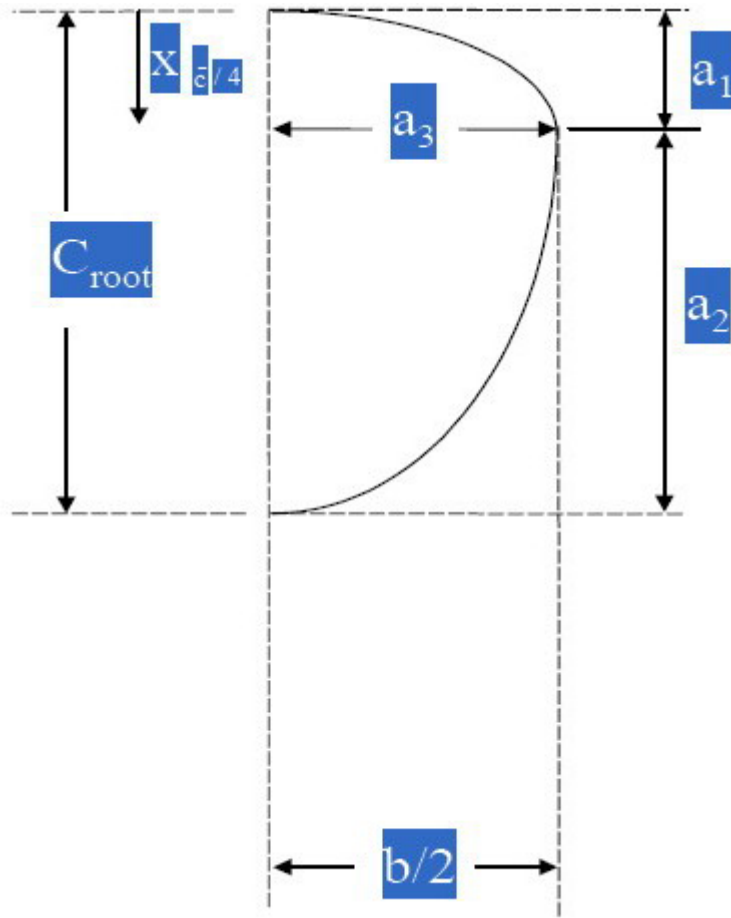
Figure 2.9 ZIMMERMAN parameters

- Area of Zimmerman (inv. Zim.):

$$S = \frac{1}{2}(a_1 + a_2)a_3\pi$$

- Plan form if Zimmerman is drawn by:

$$C(y) = (a_1 + a_2)\sqrt{1 - \frac{y^2}{a_3{}^2}}$$

- The tested platforms according to the study were:

AR	Rectangular	Zimmerman	Inv. Zimmerman	Elliptical
0.50				
0.75				
1.00				
1.25				
1.50				
1.75				
2.00				

Figure 2.10 Plan forms used in the searched studied paper

CHARACTERISTICS OF LAR WINGS AT LOW R^e

AR	Designation	C_{root} (in)	Span (in)	a_1 (in)	a_2 (in)	a_3 (in)	Area (in^2)	$\bar{c}$ (in)	$x_{\bar{c}/4}$ (in)
				Rectangular Planform					
0.50	rect0.50	8.000	4.000	n/a	n/a	n/a	32.000	8.000	2.000
0.75	rect0.75	8.000	6.000	n/a	n/a	n/a	48.000	8.000	2.000
1.00	rect1.00	8.000	8.000	n/a	n/a	n/a	64.000	8.000	2.000
1.25	rect1.25	6.000	7.500	n/a	n/a	n/a	45.000	6.000	1.500
1.50	rect1.50	6.000	9.000	n/a	n/a	n/a	54.000	6.000	1.500
1.75	rect1.75	6.000	10.500	n/a	n/a	n/a	63.000	6.000	1.500
2.00	rect2.00	6.000	12.000	n/a	n/a	n/a	72.000	6.000	1.500
				Zimmerman Planform					
0.50	zim0.50	8.000	3.142	2.000	6.000	1.571	19.739	6.791	0.552
0.75	zim0.75	8.000	4.712	2.000	6.000	2.356	29.609	6.791	0.552
1.00	zim1.00	8.000	6.283	2.000	6.000	3.142	39.478	6.791	0.552
1.25	zim1.25	8.000	7.854	2.000	6.000	3.927	49.348	6.791	0.552
1.50	zim1.50	8.000	9.425	2.000	6.000	4.712	59.218	6.791	0.552
1.75	zim1.75	8.000	10.996	2.000	6.000	5.498	69.087	6.791	0.552
2.00	zim2.00	8.000	12.566	2.000	6.000	6.283	78.957	6.791	0.552
				Inverse Zimmerman Planform					
0.50	ziminv0.50	8.000	3.142	6.000	2.000	1.571	19.739	6.791	1.157
0.75	ziminv0.75	8.000	4.712	6.000	2.000	2.356	29.609	6.791	1.157
1.00	ziminv1.00	8.000	6.283	6.000	2.000	3.142	39.478	6.791	1.157
1.25	ziminv1.25	8.000	7.854	6.000	2.000	3.927	49.348	6.791	1.157
1.50	ziminv1.50	8.000	9.425	6.000	2.000	4.712	59.218	6.791	1.157
1.75	ziminv1.75	8.000	10.996	6.000	2.000	5.498	69.087	6.791	1.157
2.00	ziminv2.00	8.000	12.566	6.000	2.000	6.283	78.957	6.791	1.157
				Elliptical Planform					
0.50	ell0.50	8.000	3.142	4.000	4.000	1.571	19.739	6.791	0.855
0.75	ell0.75	8.000	4.712	4.000	4.000	2.356	29.609	6.791	0.855
1.00	ell1.00	8.000	6.283	4.000	4.000	3.142	39.478	6.791	0.855
1.25	ell1.25	8.000	7.854	4.000	4.000	3.927	49.348	6.791	0.855
1.50	ell1.50	8.000	9.425	4.000	4.000	4.712	59.218	6.791	0.855
1.75	ell1.75	8.000	10.996	4.000	4.000	5.498	69.087	6.791	0.855
2.00	ell2.00	8.000	12.566	4.000	4.000	6.283	78.957	6.791	0.855

*All models have zero camber and thickness of 5/32 in. The thickness to root-chord ratio is 1.96% for the 8-inch chord models and 2.60% for the 6-inch chord models

Table 1 Characteristics of wings tested in the study

2.3 Results of the Study

Study Observed a "kink" in the C_L vs. angle of attack curve at $R_e = 70,000$ and non-linearity but this problem seemed to be no longer apparent at higher R_e.
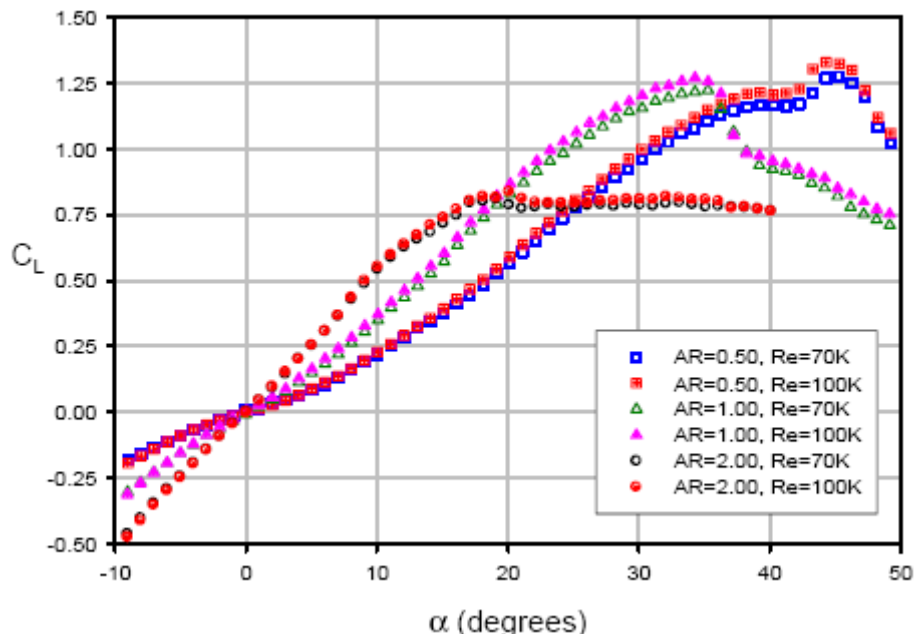
Figure 2.11 C$_L$ vs. α, Rectangular Plan form, Effect of Re
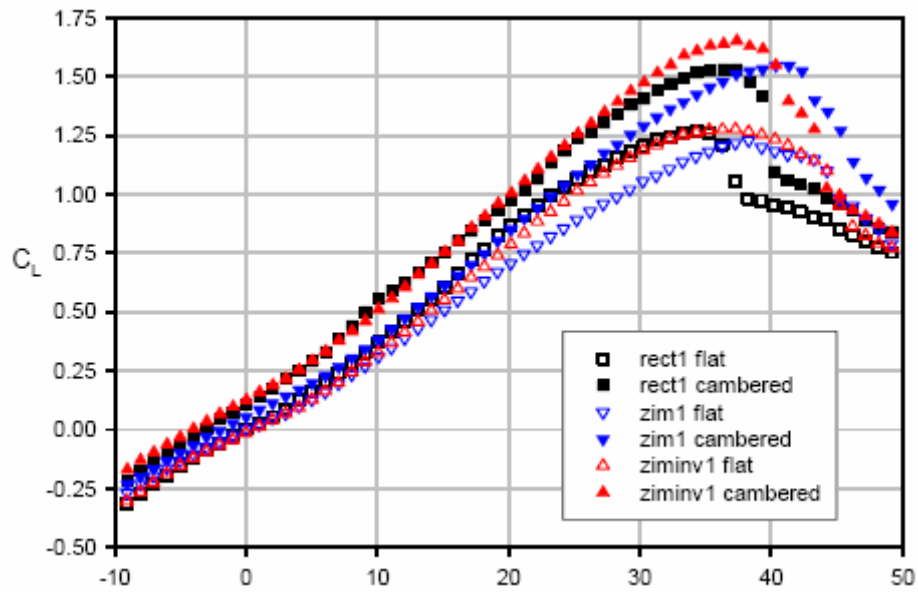
Figure 2.12 C$_L$ vs. α, AR = 1.00, Effect of Camber, Re = 100,000
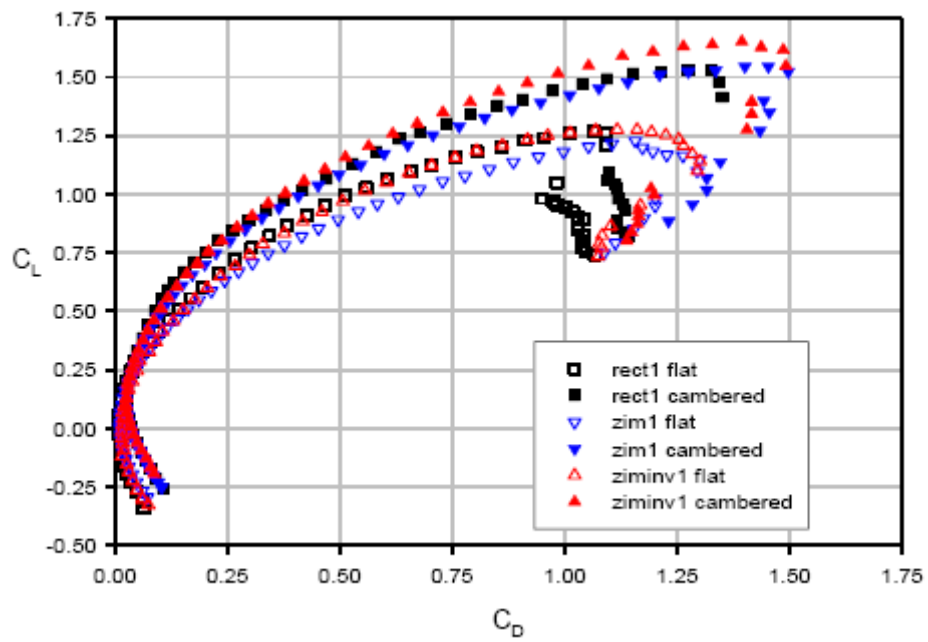
Figure 2.13 C$_L$ vs. C$_D$, AR = 1.00, Effect of Camber, Re = 100,000
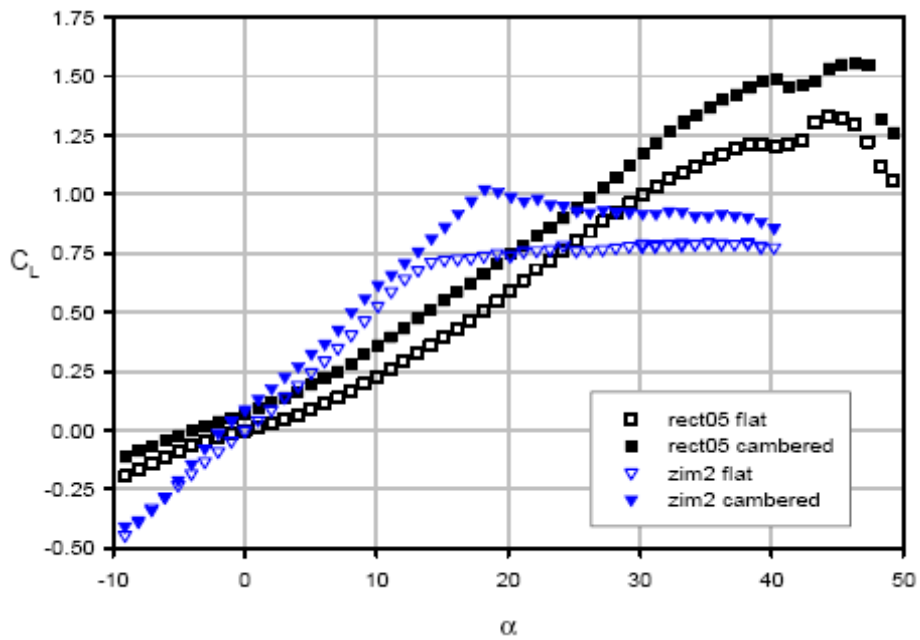
Figure 2.14 C$_L$ vs. α, AR = 0.50 and 2.00, Effect of Camber, Re = 100,000
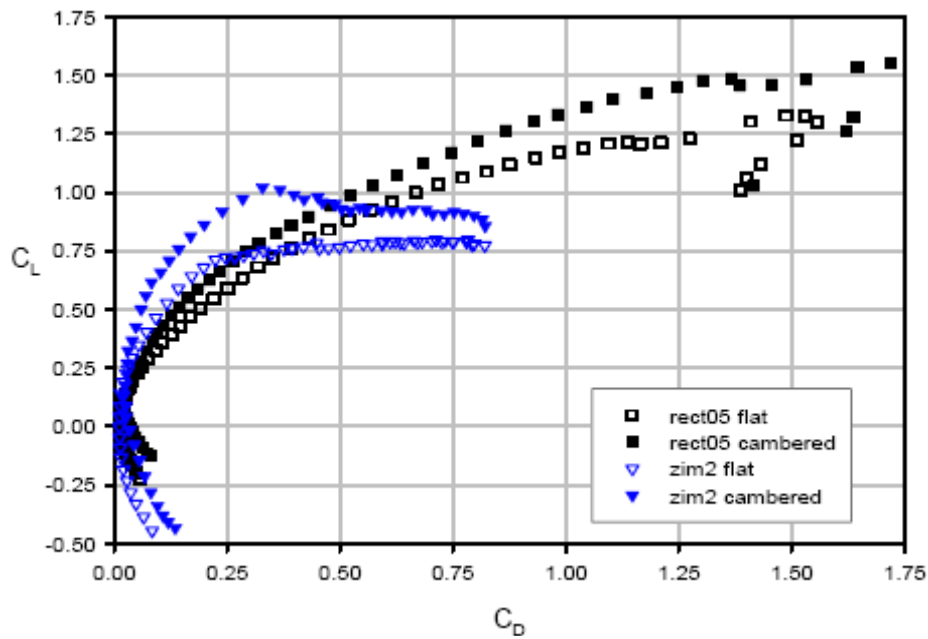
Figure 2.15 C_L vs. C_D, AR = 0.50 and 2.00, Effect of Camber, Re = 100,000

From the study and its curves it can be concluded that the rectangular and inverse-Zimmerman wings performed the most efficient. However, inv. Zimmerman wings showed higher L/D ratios while operating at low at low R_e ranging between 70,000 – 140,000 and low AR's.

Study suggested that the effect if the plan form is more analyzed when plotting C_L vs. $X_{\max span}$. $X_{\max span}$ is a chord-wise location (measured from L.E.) of the max wing span, non-dimensionalized by the root chord of the model. $X_{\max span}$ were as shown in the table below:

WING MODEL	$X_{\max span}$
Zimmerman	0.25
Inv. Zimmerman	0.75
Elliptical	0.5
Rectangular	1

Table 2 $X_{\max span}$ **of different wing models**

$X_{max\,span}$ provides an indirect measure of distance between the wing-tip vortices as they develop over the wing and travel down stream. It was found that the distance between the wing tip vortices varied proportionally with the chord-wise location of max span.

Hoerner & Borst suggested that lift performance of low AR wings improved as the distance between the wing-tip vortices increases.

The paper illustrated the separation bubbles:

- A separation bubble occurs when laminar flow near the L.E. of a wing separates from the wing surface.

- The width of the separation bubble can vary from a few percent of the chord to 20% or 30% of the chord.
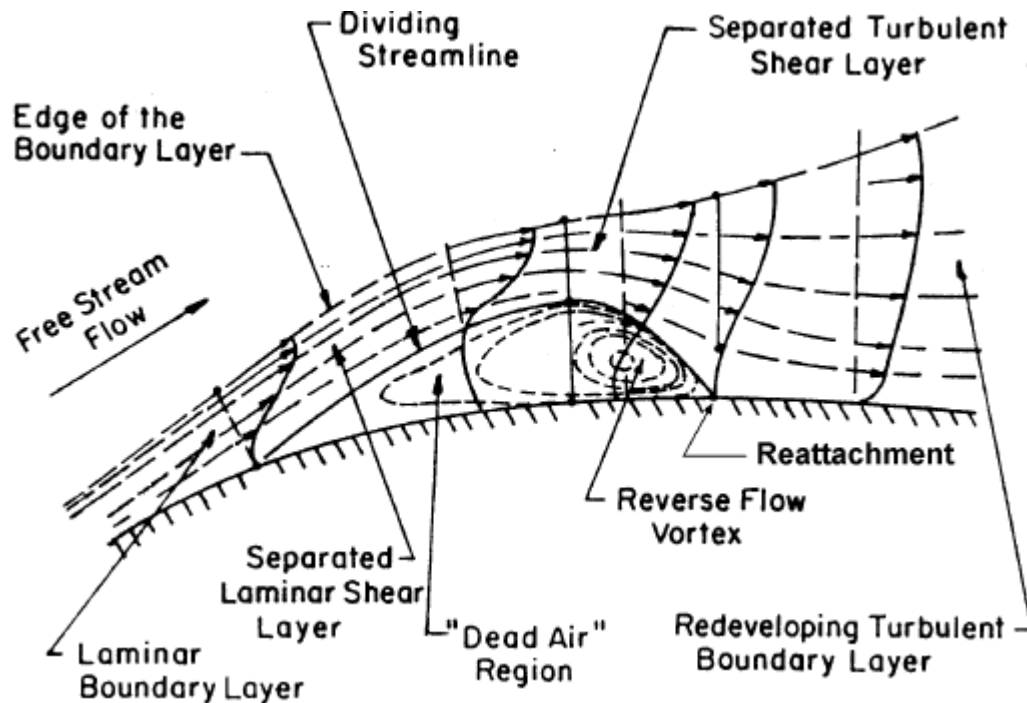
Figure 2.16 Schematic of a Separation Bubble

2.4 Conclusion

The study established a firm understanding for the aerodynamic case and data extracted from it provided a solid base for the MAV design as it was extracted from practical experiments and tests. However, the MAV wing's airfoil is still an issue that should be researched to build the first MAV prototype.

3 CHAPTER TWO: DESIGN CRITERIA FOR ENDURANCE MAV

3.1 Introduction

Typical designs for MAVs are the Endurance MAV and the Surveillance MAV. In order to have a proper design for the project's MAV, the team needed a certain criteria to follow as a reference. An annual competition is set in the USA for academic and research organizations to compete on the two MAV design concepts. This competition's criteria were taken as a reference. According to this competition the Surveillance and Endurance MAVs were defined as follows:

3.2 Surveillance MAV

Surveillance MAVs are appreciated according to its ability to identify a target on the ground from a certain altitude.

According to the annular MAV competition, Surveillance MAV should identify a target 600 meters away from the launch site. The target specifications are:

- A letter or number 1.5m x 1.5m in size

- Enclosed by a 3.5m x 3.5m fence, 1.5 meters in height

Typical target acquisition flight duration is less than one minute. Thus, the efficiency of the surveillance MAV is not a large factor in the design. Rather, it is more important to have a stable platform that maintains consistent video stream for the projected flight time of one minute. The performance of the MAV is based on three main design characteristics:

- Minimal wing loading

- Lateral and longitudinal stability

- Maximum lift to drag ratio

3.3 Endurance MAV

The endurance MAV airframe is designed to have the smallest dimension, while flight systems are optimized to attain the maximum flight time. Lightweight components are used to minimize the wing loading, which then allows for a smaller MAV.

Endurance MAVs are appreciated according to this simple equation:

$$Score = \frac{FlightTime(s)}{[MaximumDimension(cm)]^3} \dots\dots\dots\dots\dots\dots\dots(*)$$

According to the annual MAV competition

Design Criteria: Endurance MAV

$$Score = \frac{8.31 \times 60}{(6 \times 2.54)^3} = \frac{498.6}{3539.606}$$

$$\therefore Score = 0.140863$$

This project is focusing on endurance MAV in an indoor flight as a main challenge. This chapter is to focus on MAVs development through the improvement in CFD/Wind tunnels tests, propulsion systems, and control systems.

Project's MAV is based on those objectives:

1. Endurance MAV with the mission of flying the longest period of time.

2. MAV should have max dimensions of 6 inches × 6 inches.

3. MAV should be stable in indoor flight and have acceptable maneuver

4. Capabilities.

5. Weight is much of a consideration to allow later study of adding more payloads as cameras to develop MAV for surveillance missions. Max components weight is 66.6 grams.

3.4 Aerodynamics

Aerodynamics study of the project was considered in the previous chapter. According to this study, Inverse Zimmerman plan forms were found to give the best results when avoiding using aspect ratios close to 0.5 or less.

Aerodynamic tests for the project are discussed in a following chapter. Tests are based on CFD tests on ANSYS CFX package. Depending on this package, tests were made for several configurations.

3.5 Propulsion

The design of the propulsion system for the endurance MAV is based on propeller and motor optimization. In addition, motor technology has been a limiting factor in the size of MAVs. Thus, the most suitable of motors are chosen based on weight, efficiency, and availability. So, a combination of motors and propellers were considered. Motor chosen was an electric motor, a brush-less one for its relative high efficiency and light weight beside its low noise. Also brush-less motor was chosen for its sufficient thrust.

Design Criteria: Endurance MAV

As for the propeller, no design was made for it; instead, we just purchased a suitable one for the chosen motor.

3.6 Conclusion

This year's MAV research at Cairo University tried to focus on development of endurance MAV. Surveillance for components and optimizing the chosen components has been made. Design for the airframe and study of manufacturing it was made. Testing designed airframe on CFD package to get a design point was also done. Work was made to show that for a first MAV project at Cairo University and maybe in Egypt's Engineering academic organizations was worth it.

3.6.1 Computing score for project's MAV

BATTERY CAP	*300*	*MAH*
Battery volt	*3.7*	*v*
motor volt	*3.5*	*v*
motor current	*2.29*	*amps*
Battery power (watt hr)	*1.11*	*watt hr*
motor power	*8.015*	*watt*
Battery discharge time	*0.13849 (hr)*	*8.30942 (min)*
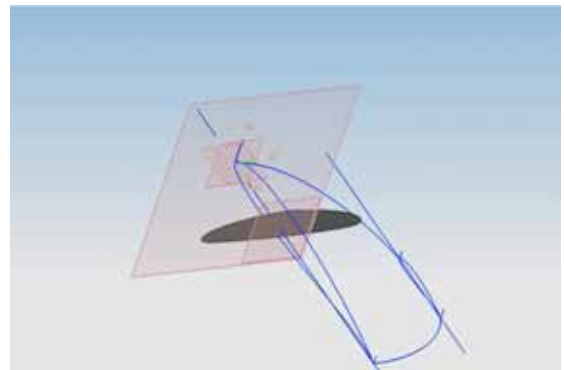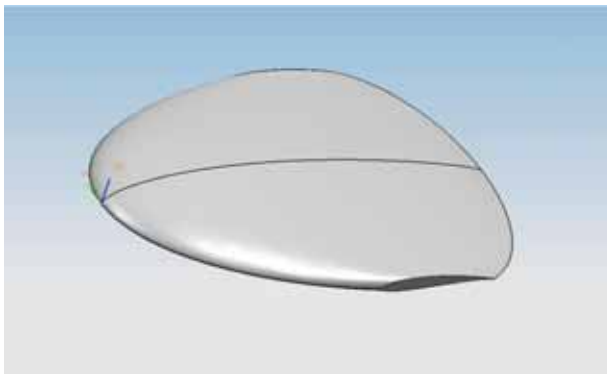
Figure 3.1 Designed wing, Sections in designed wing

4   CHAPTER FOUR: COMPUTATTIONAL FLUID DYNAMICS ANALYSIS

This chapter handles the computational analysis done to predict the flow characteristics of our MAV design under different flight conditions and angles of attack. The solver used was a ready built package developed by ANYS called CFX. Several tests were carried out with the software to select the best solver model. Furthermore, two designs were compared to choose the final production model.

4.1   Modeling

In this section we discus the process of creating the graphical computer models that would go on to be analyzed. Both modeling and meshing were conducted using another software package developed by ANSYS called ICEM. This allowed for convenience in terms of software compatibility and an uneventful transition between meshing tool and solver.
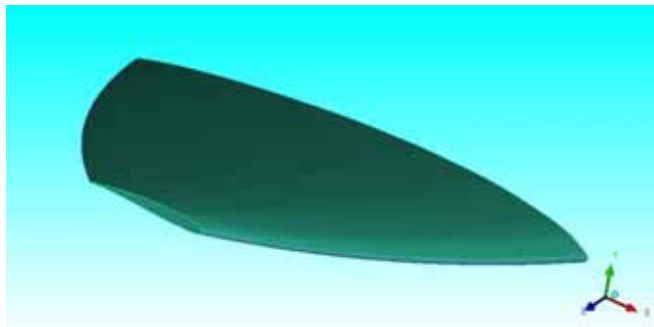
Figure 4.1 Half-wing geometric model

4.1.1   Plan form modeling

Our decision for the vehicle plan form profile was the inverse Zimmerman geometry. To accomplish this, a set of points were created in to the modeler. The points were created at different chord stations a long the edge of the plan form. This was done by feeding the plan form equations in to the multiple-point tool in the software.

After the point generation phase, a poly line was created to connect all the points producing the Zimmerman plan form.
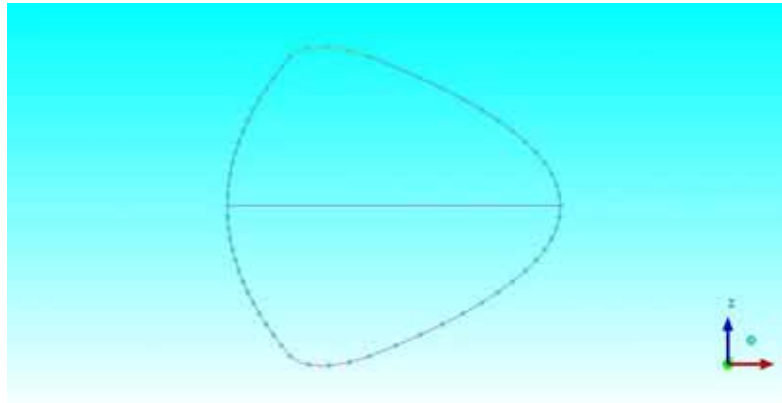
Figure 4.2 plan-form point distribution

Some trials were carried out to create a 3D variation of the plan form; however it served no purpose to the design but was simple to prepare for adding the airfoil section.

4.1.2 Airfoil modeling

Creating the model for the airfoil was done in much the same way the plan form modeling, however there were no equations available for the profile and one had to be created first. This was only done for the Eppler 212, as the modified Eppler had an equation.

The E212 was defined as a set of coordinates given in a data file. To create an equation for use in the multi-point tool, the points in the data file were inputted into MATLAB and a poly-fit function was used to produce two 4th order polynomials describing both upper and lower thus of the airfoil.

As mentioned earlier, 2 airfoils were tested computationally; a thin modified Eppler comber line and an Eppler 212.

4.1.2.1 Thin airfoil

This airfoil was developed by a group working on a MAV as well. They used a special computer code to produce an extension to the Eppler trailing edge to stabilize their flying wing. The code produced a 6th order polynomial, which defined a comber line.

We directly imported the polynomial function, taking care to adjust it to draw the airfoil with our chosen chord length.
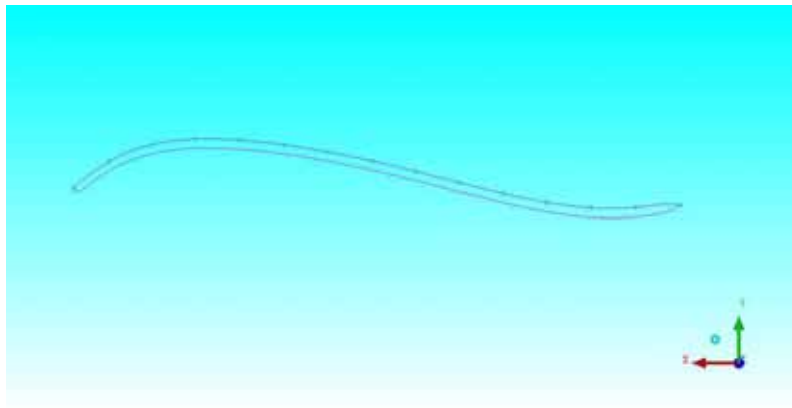
Figure 4.3 Modified Eppler camber line with uniform thickness

The points resulting from the function produced a line which needed to be given a thickness. This was done by creating an offset of this airfoil in the same vertical plane, 4mm was the chosen thickness, and the edges of both profiles were connected using semi circular lines.

4.4Figure Thickness added to camber line

4.1.2.2 Thick airfoil

The thick airfoil, Eppler 212, was fully drawn using the functions mentioned further up. No offset was needed as the functions fully defined the perimeter of the airfoil.
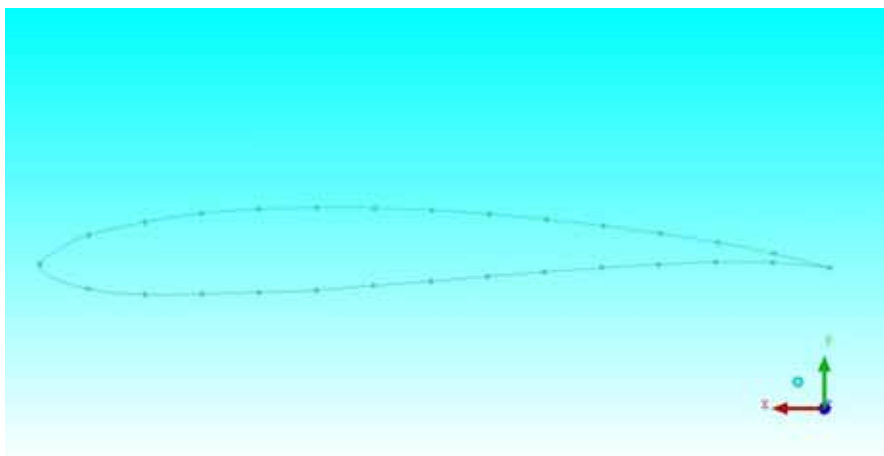
Figure 4.5 Eppler 212 point generation

4.1.3 Wing tip

An issue that had occurred was how the wing tips profile should be chosen. Several options existed, and in our case 3 main presented themselves. The first was to have the thickness decrease linearly from the root towards the tip where it would reach zero.

The second option was to preserve the airfoil aspect from root to tip. This was done by selecting a certain minimum chord length, after which the tip was trimmed off. This span wise station, an airfoil was drawn using the above mentioned chord length.

The third option, although was not modeled, still was tested during the construction phase. This was to have the tips fold upwards to create small vertical fins, these would serve as to reduce tip vortices and stabilize the aircraft laterally.
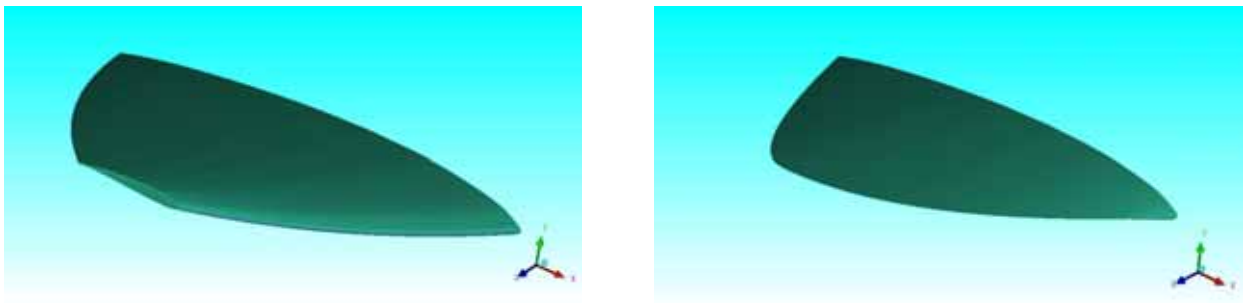
Figure 4.6 Tip geometry resolution

The solid was modeled by simply creating surfaces between the plan form and the different airfoils.

The simulation domain was also modeled to create the required boundaries. 6 surfaces formed the domain bounding box. The dimensions were selected such that each surface it at least 3 chord lengths from the MAV. Conventionally due to limited computer resources, this reduction would reduce mesh size and hence the processing cost with, minimum accuracy loss.

A final note, to allow for greater mesh sizes using the same resources, the wing symmetry was used. To elaborate, each simulation domain and wing configuration was modeled as both full span and half span.
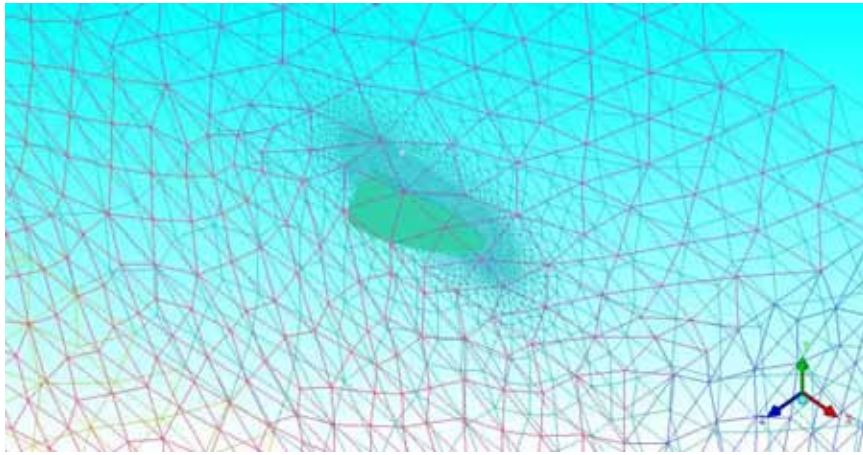
Figure 4.7 Half-domain mesh example

4.2   Mesh generation

Mesh generation, also referred to as meshing, is the process of creating the 3-dimensional grid of volumetric elements over which a computational solution of the fluid flow is to be calculated, meshing can be a somewhat challenging process because one tries to achieve the best balance between solution accuracies, computational cast, convergence speed and geometric watching.

4.2.1   Element type

The meshing elements used were tetra-type elements, with prism-type elements used on wing surfaces to capture boundary layer. In the mast cases no surface meshing was used before moving on to volume meshing. However, whenever volume meshing at certain size and configuration failed to capture any geometric feature surface mesh was created.

4.2.2   Initial mesh generation

Initially, trial meshing around the different geometrical to detect and understand the problems out particular presented. It was found that there was a mesh size needed after which the geometry was not represented with acceptable accuracy. Furthermore, we were able
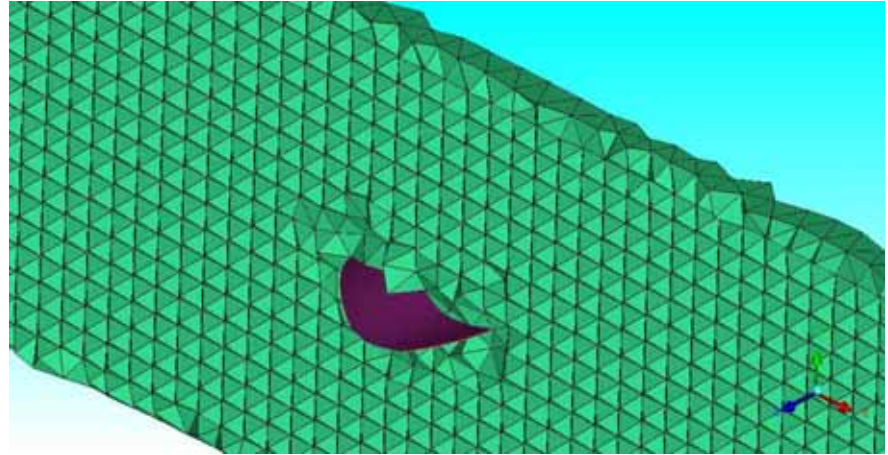
Figure 4.8 Un optimized mesh section over thin airfoil

to find the number of elements after which the computer was unable to carry out operation due to resources overload. This occurred after the element count reached over 1500000 elements.

After the initial trials, a number of mesh sets were created for each geometric configuration with increasing number of elements. This was needed to confirm solution consistency as increasing number of elements should show a converging solution value.
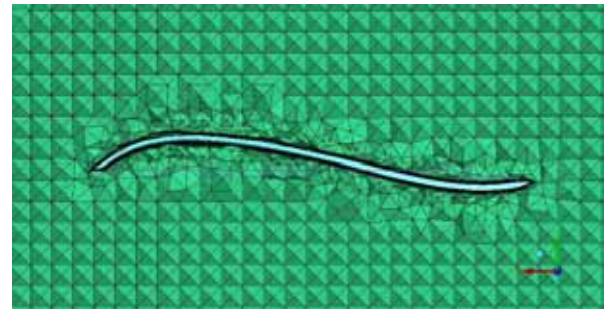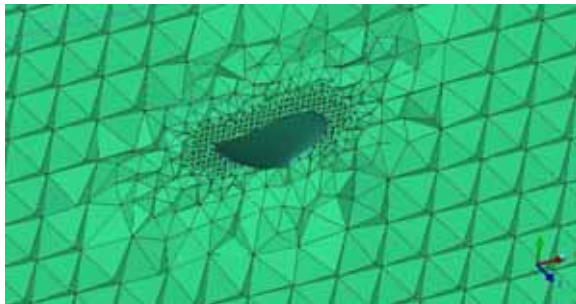
Figure 4.9 Optimized mesh distribution over thin airfoil

4.2.3   Mesh optimization

Having created the mesh sets, we moved on to optimization which meant using the number of elements to capture the areas of concern with the greatest possible accuracy. To accomplish this, mesh density was used. Mesh density is a feature in the software that allowed a higher density is a feature in the software that allowed a higher density of elements (i.e. small sized) to be allocated around areas of rapid change as desired. This essentially translates to a better solution for the same number of elements.

The last step was to create prism elements to capture the boundary layer. Prism elements are elements of small heights that can be stacked close to surfaces to detect fluid changing variables with normal distance from surface.

4.3 Solution Phase

In this section we will discus the preparation and process of computational solution of the meshes handled in the previous

Figure 4.10 Prism meshing elements over geometry surface

sections. Preparation of the domain type, solver type, etc… The process refers to the actual progress of the different computational runs in terms of convergence properties and termination.

4.3.1 Solver Information

The solver we used for the analysis, as mentioned before, is ANSYS CFX 10.0. Due to the fact that this is a ready built package, information about the mathematical schemes and inner-workings of the solver code are scarce.

4.3.2 Preparation

The software allows easy problem setup through a graphical user interface referred to the PRE-engine. To begin we imported the geometry and mesh from our previous work. Problem scale was checked and the geometry condition was also checked to ensure no errors occurred during import.

Next, the domain type was selected and the parameters initialization. This would be a constant through all the analysis. A fluid domain was selected as the type with Air Ideal gas as the fluid. The reference pressure was taken at 1 atm and the domain mobility was set as "stationary domain".

Furthermore, the simulation type was set as steady state. The energy model chosen was isothermal given that no heat exchange of considerable order was expected and the system temperature was set at 300 K. this temp represented room temperature where the MAV was expected to operate.

Other models existed, however they were not used. These included reaction model, thermal radiation model and discontinuity models (sources and sinks).

4.3.3 Turbulence Model

Due to the scale of the problem combined with the low Reynolds number involved, choosing a suitable turbulence and viscosity model proved challenging. The main requirement for the model was to allow for fairly sensitive boundary layer transition selection. Also it needed to have no assumptions in its formulation that put a condition on the Reynolds number.

CFD
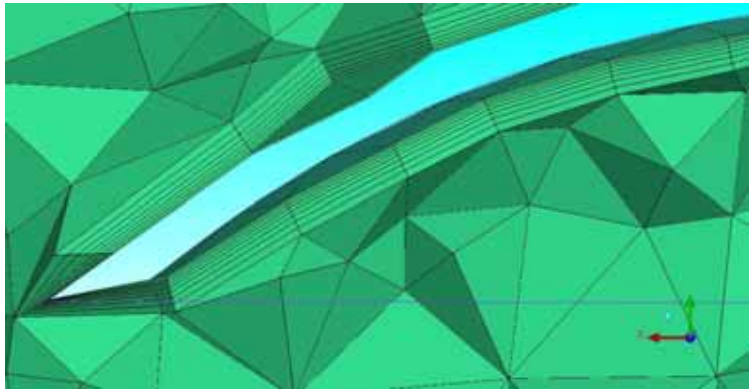
ANSYS documentation recommended a 2-eqaution shear stress transport model that could be coupled with another 2-eqaution gamma-theta model for detect boundary layer transition. This recommendation, however, concerned low Reynolds number problems than ultra low ones.

To quantify the issue, several extra runs were prepared for a selected flow condition, each with a different viscosity model. The models tested were as follows:

- A 7-equations Reynolds stress model,

- A 0-eqaution laminar flow model.

- Shear-stress transport model.

4.3.4   Boundary Conditions

During the modeling phase, we selected a 6-sided domain geometry, which means that we had 6- Boundaries for the problem.

Since the computational analysis planned would be concerned with longitudinal performance, the two boundaries on either side of the wing were considered walls with a free slip condition, thusly representing far stream.

Moving on to inlets, these depended on the angle of attack, and accordingly so did the outlets.

For positive angle of attack, the front and the bottom domain sides would be the inlets, and the opposing surfaces would be outlets. In the case of negative angle of attack, the upper domain side would be inlet and bottom an outlet.

Inlet boundaries were setup using Cartesian velocity components. This allowed angles of attack to be inputted without changing problem geometry. The entering flow was further initialized with 5% turbulence magnitude.

Outlet boundaries were initialized as domain openings. The condition enforced at these openings was zero static pressure. This condition did not alter flow velocity, as the velocity was expected to redistribute due to the wing disturbance. Moreover, zero static pressure meant the flow average velocity returned to inlet value.

For the symmetric geometry problems, the symmetry surface had a unique boundary condition; symmetry.

A final boundary condition was set on the wing itself. The wing was set as a wall boundary with No Slip allowed over its entire surface.

4.3.5   Initial condition and solver control

There were only one inlet conditions enforced. The first was on flow velocity, the entire domain was given the flow velocity of the inlet, without any angle of attack. This served as to jump start the solver and decrease analysis time.

The second initialization parameter was turbulence eddy dissipation, which we let the software initialize automatically.

CFD

Solver control included a large set of parameters. However, we were only concerned with the termination criterion; all other parameters were left as their defaults. Our termination criterion was as follows:

- 100 iterations

- 10^{-4} mass and momentum RMS errors

In some cases, we manually terminated the solver runs; this was done when momentum errors converged to a higher value than 10^{-4} bout other flow variables errors converged to a satisfactory value.

4.4 Results

The preliminary set of computational runs was conducted to test mesh density versus solution accuracy. Another set of runs followed using the meshes selected from the first set to compare the two airfoils used. Other complementary runs were concluded to test turbulence models, the effect of using a heat exchange model and the effect of changing tip geometry. The results for these runs will be discussed in this section.

4.4.1 Mesh vs. Accuracy

The data collected from varying mesh size revealed a couple of interesting features. We used the value of the zero angle of attack lift as a benchmark for comparison.

The full span meshes seemed to converge to a certain value with decreasing difference between each two sizes. The convergence was somewhat linear, and it approached from higher values moving to lower values.

The symmetric mesh model showed pretty much the same convergence characteristics, however, the approach was inverted, that's to say, moving from lower values to the convergence line. The symmetric model performed favourably in terms of computational speed and the solution consistency.

At the end of this comparison, it became clear that although the symmetric mesh would limit the analysis to longitudinal flow, the speed trade-off was well worth it. The mesh size we used was selected so that the benchmark difference with the finer mesh would be less than 8%.

4.4.2 Eppler Mod Vs. 212

We went to use the symmetric mesh for both airfoils, each with the following specifications:

Airfoil	Theta	Prism	Span	Max. chord	Camber	Thickness
E212	606314	59408	14.0	15.0	4.2	0.23
E mod	711236	69216	13.8	14.8	0.66	1.58

The runs were conducted for a free stream velocity of 25 m/s and angle of attack varying from -2.5 to 15 degree.

4.4.2.1 C_l vs. Alpha
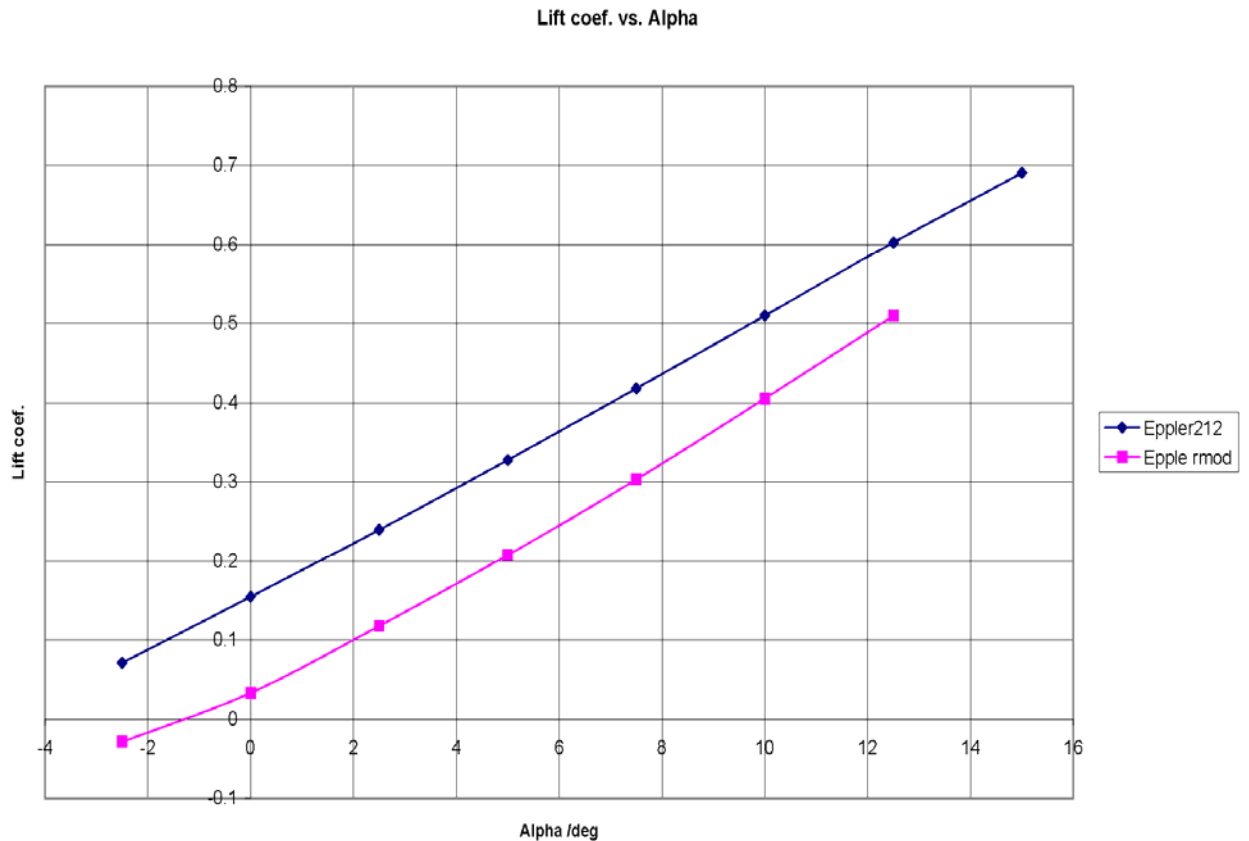
Figure 4.11 Comparison between Cl values of E212 and mod. Eppler

The lift coefficient of the Eppler 212 showed a significant advantage over the modified Eppler. However, the modified Eppler had a slightly higher gradient. The difference in lift can be attributed to the loss in lift force that occurs in the modified Eppler due to the reflex section at the trailing edge, as well as the absence of a thickness distribution. In chapter 2, the study mentioned that at lower Reynolds' numbers, the effect of thickness is much less pronounced.

4.4.2.2 C_{mLE} Vs. Alpha
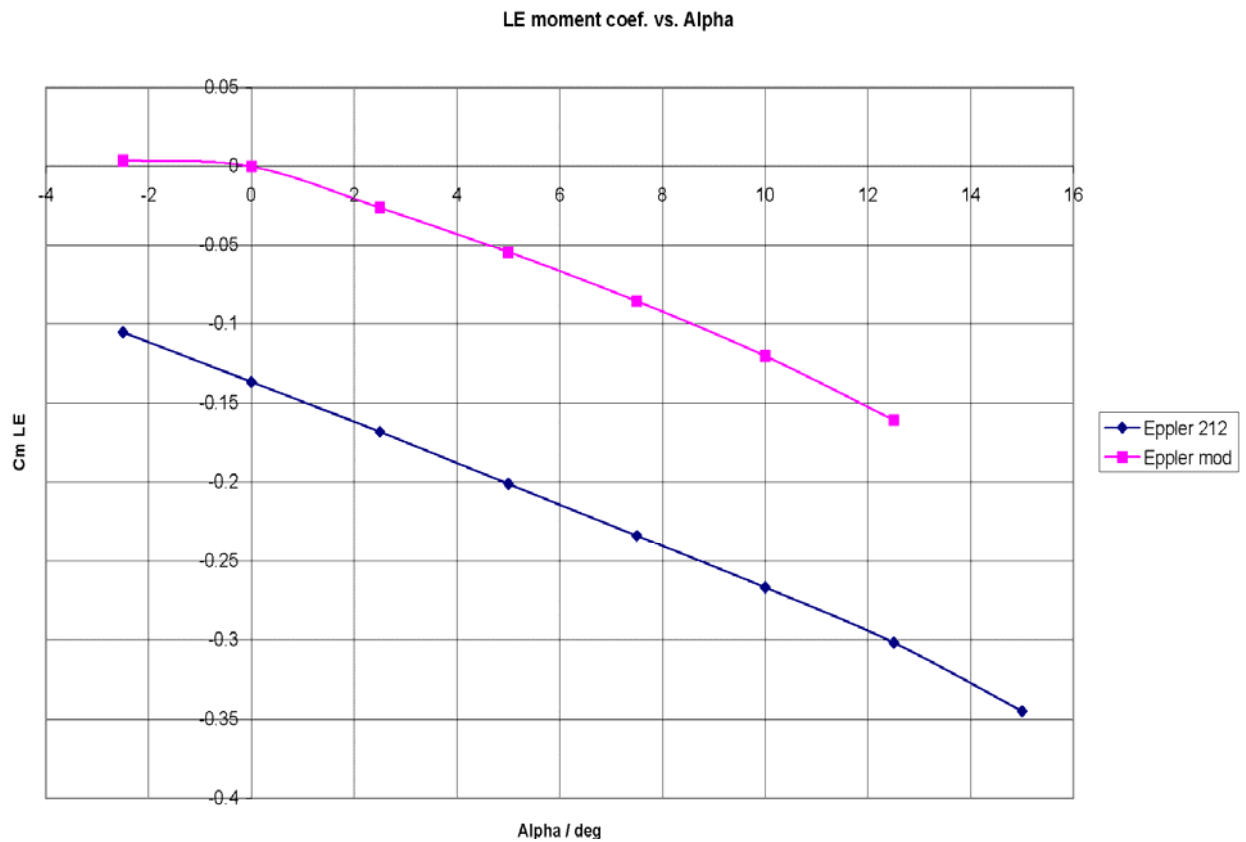
Figure 4.12 Comparison between leading edge Cm values for E212 and mod. Eppler

From this leading edge moment coefficient graph, it is apparent that the modified Eppler outperforms the E212. The former has a much more positive zero angle of attack pitching moment, owing to better stability for a flying wing. This is a direct result of the reflex trialing edge characteristic of the airfoil.

4.4.2.3 Cl vs. Cd
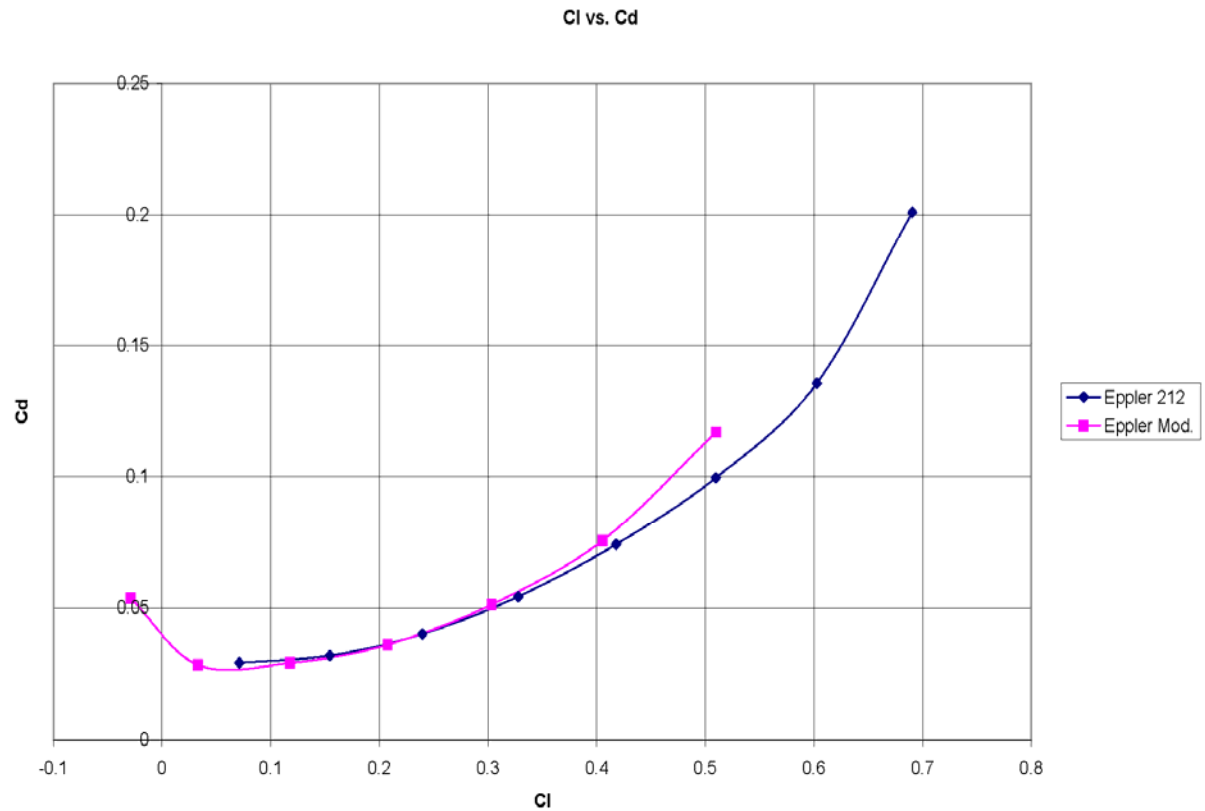
Figure 4.13 C_L Vs. C_D for both airfoils

These results show a slightly higher maximum value of C_L/C_D for the E212 airfoil.

It is important to note that during this solution phase we were not concerned with the solution parameters of the MAV airfoils. Therefore the velocity was not varied.

We were concerned, however, mainly with lift and drag values. In these categories the E212 excelled producing a significantly better lift curve.

The modified Eppler did excel in one area, and that was the pitching moment, which was not a surprise as it was originally conceived with that in mind. It produced a significantly more positive zero angle of attack moment.

Our decision was still more strongly influenced by the lift provided, leaving the moment problems for the stability analysis phase, during which an elevator trim would act to stabilize the wing.

4.4.3   Performance analysis of the E212 with trimmed tip

The wing tip tests computed for the e212 showed no considerable change, only a slight advantage for the trimmed tip wing. The decision then followed to go forward with the trimmed edge; this was more strongly influenced however by construction consideration.

A set of solver runs were done, varying both velocity and angle of attack:

- Velocity: 5 $\rightarrow$ 25 m/s

- Alpha: -2.5 $\rightarrow$ 15°

These produced the following results:
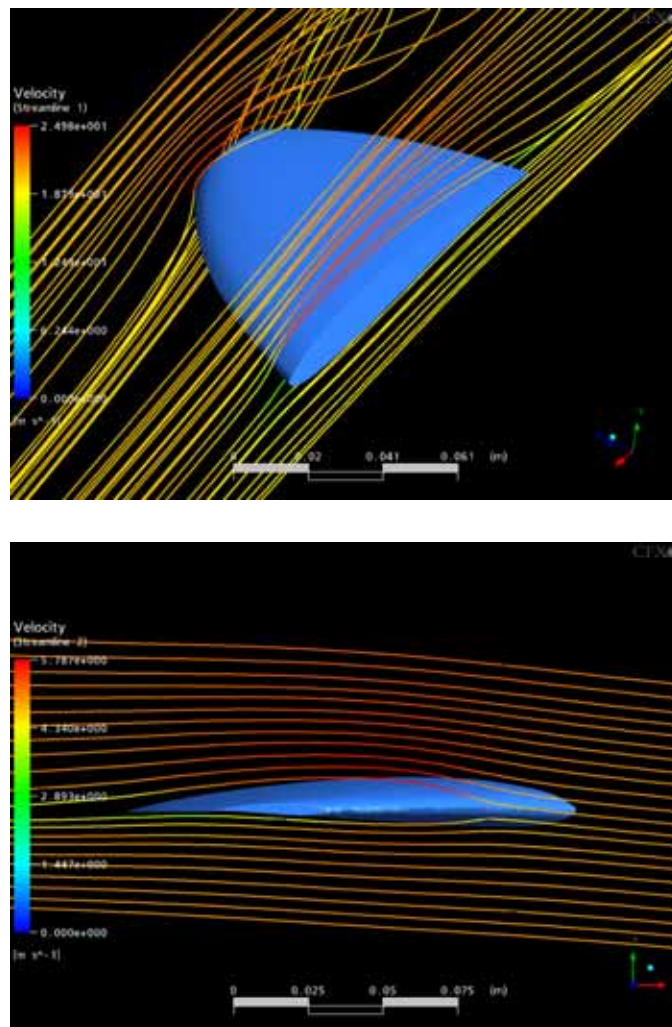
Figure 4.14 results' streamlines

51

Lift coef. vs. Alpha
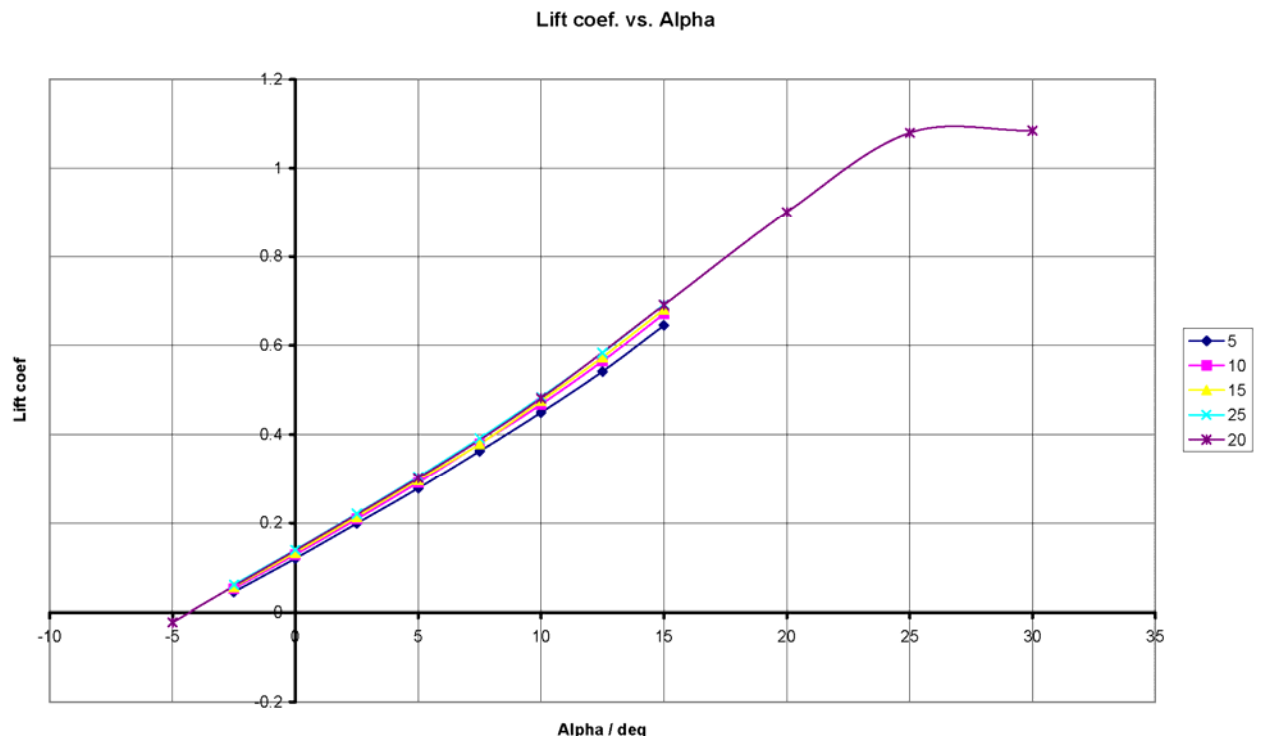
Figure 4.15 Lift Coefficient variation

After testing was finished in the stated angle of attack interval, it was found that no stall occurred up to 15°. To find the stall angle of attack, further tests were performed on the 20ms-1 flow with a new interval (-5 →30°).

The data shows a very slight drop in the gradient with decreasing flow velocity.
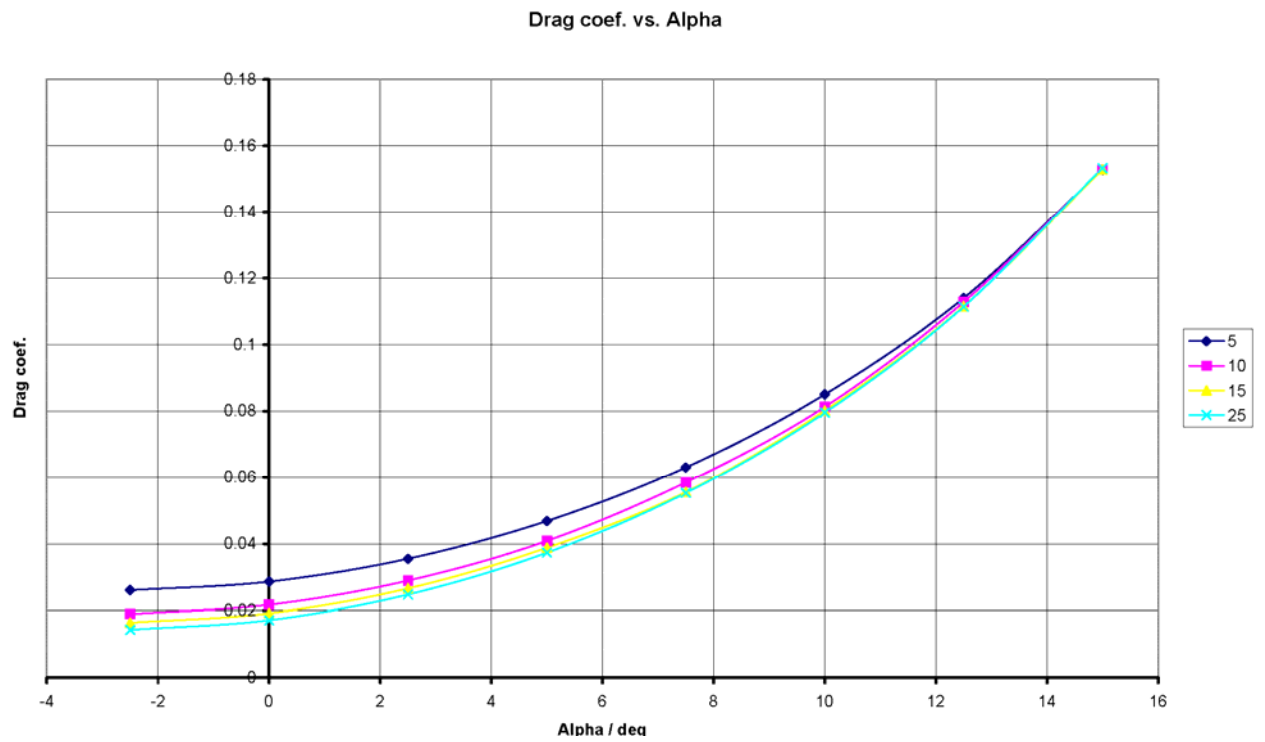
Figure 4.16 Drag coefficient variation

These curves clearly show a distinct difference in drag coefficient with decreasing angle of attack at different velocities. However, this is almost completely negated at approximately 13$^{\text{o}}$.

53

AC moment coef. vs. Alpha
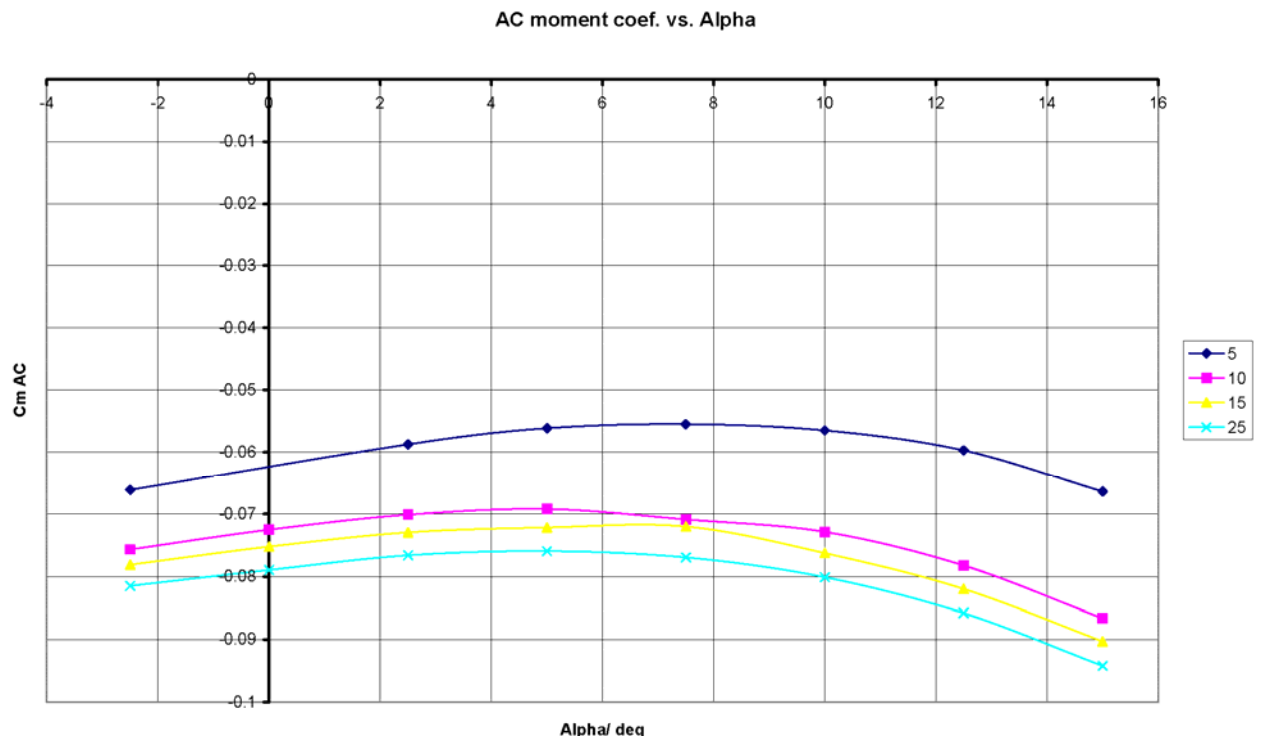
Figure 4.17 Aerodynamic center moment Variation

The value of the aerodynamic center moment coefficient seems to significantly shift upwards with decreasing velocity. It does not, however, intersect with the x-axis at all.
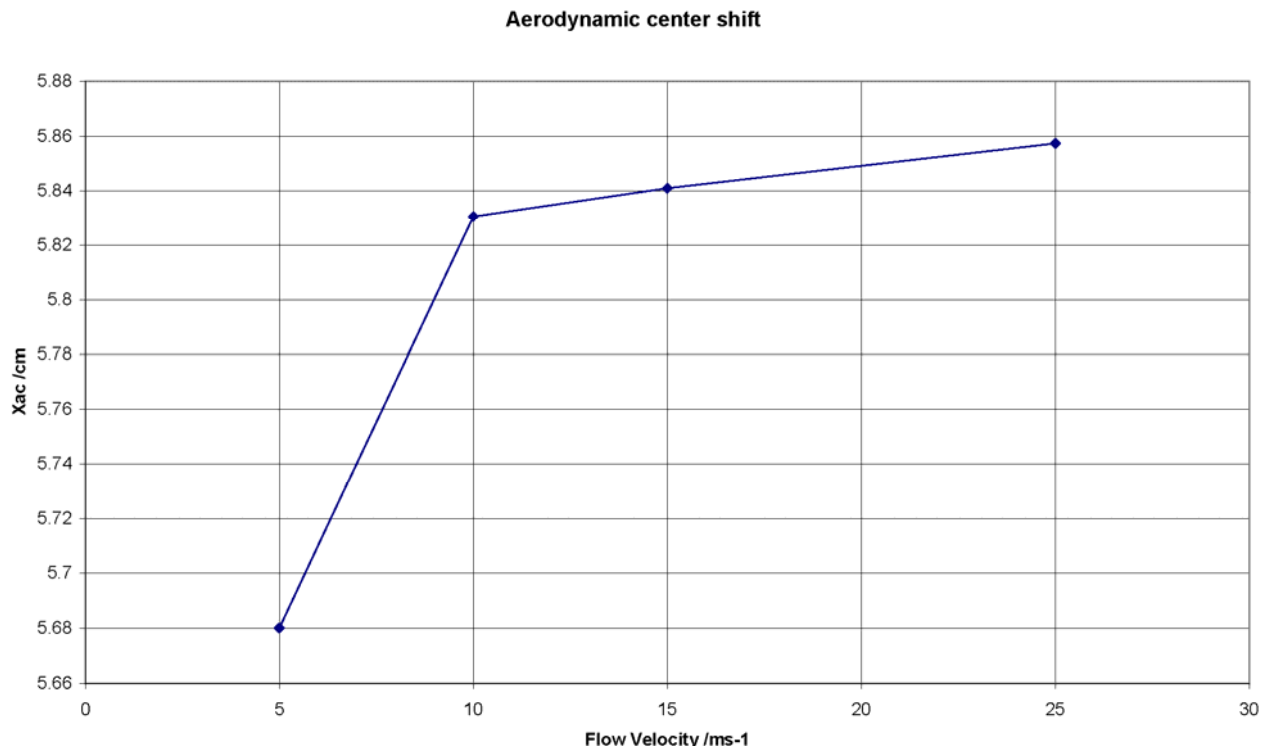
Figure 4.18 Aerodynamic center movement

The aerodynamic center of the wing shifts slightly towards the trailing edge with increasing incident velocity. The change is however small enough to neglect. It is important to note that the location of the aerodynamic center was calculated using trial and error; moment around an arbitrary place point was calculated and the point was shifted until the angle of attack variance of the pitching moment reached a minimum value.

CG moment coef. vs. Alpha
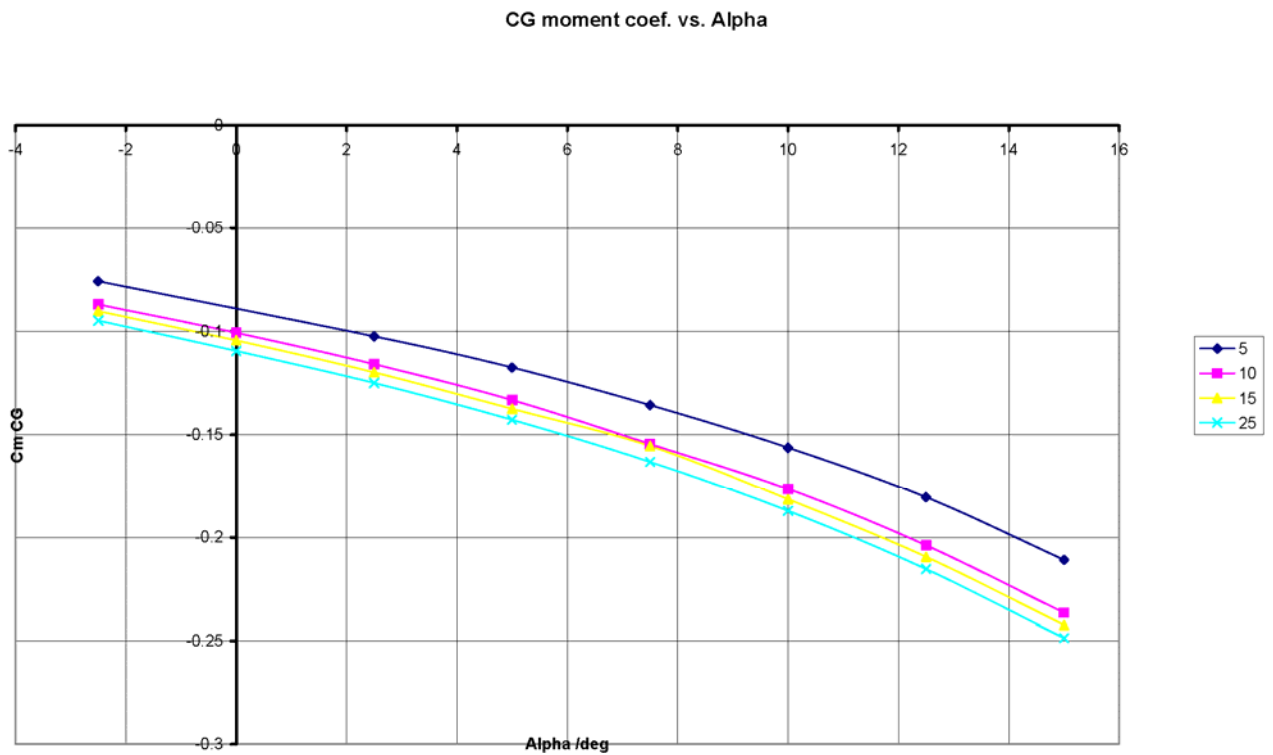
Figure 4.19 Pitching moment coefficient variation about the center of gravity

The center of gravity was assumed at a point approximately 4.8 cm from the leading edge; this was done during the design phase. From this assumption, the curves produced predict a very negative trim angle of attack. The gradient is negative; however, it is not severe. The effect of flow velocity is considerable.
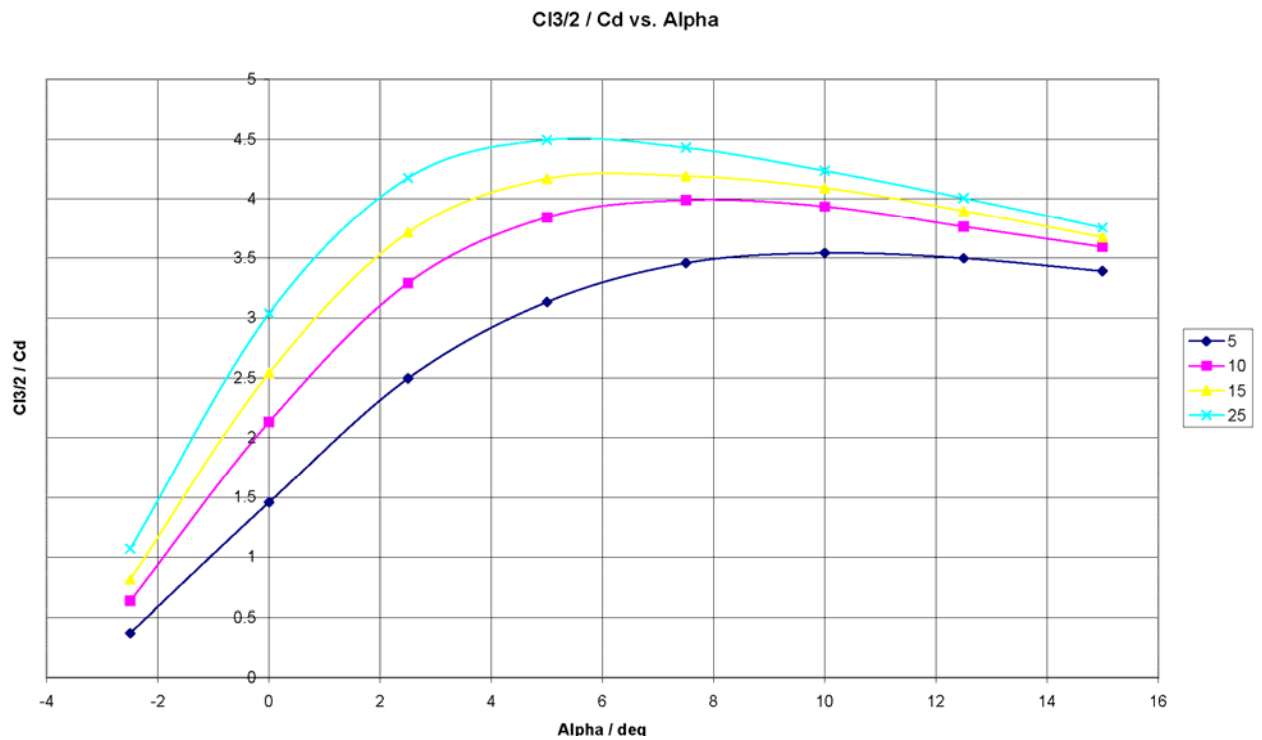
Figure 4.20 $C_L^{3/2}/C_D$ variation

$C_L^{3/2}/C_D$ is a performance analysis parameter, it concerns the maximum endurance for a propeller driven aircraft. The curves above show that the maximum value decreases somewhat with decreasing velocity. Furthermore, the angle of attack for said maximum seems to drift towards higher values with decreasing velocity.

57
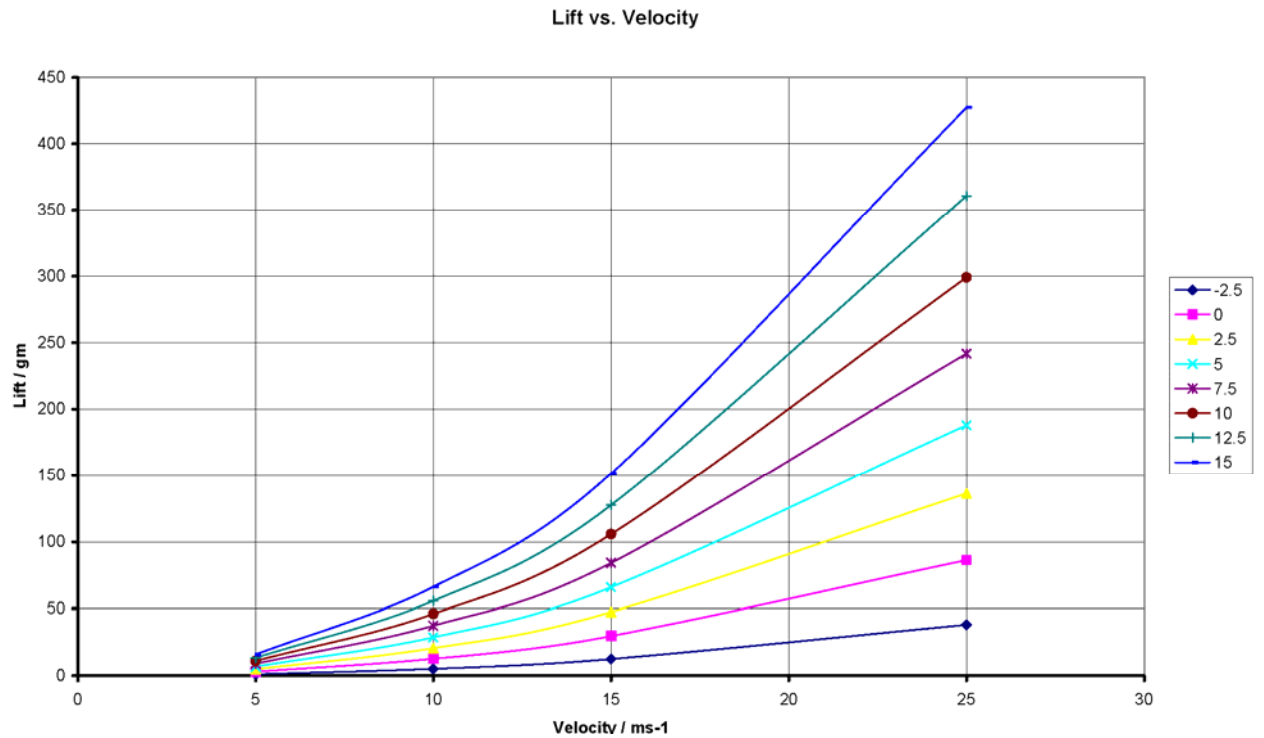
Figure 4.21 Lift variation with velocity change

This curve was drawn up in an effort to quantify the amounts of lift produced by the lift at different flow velocities. The vertical axis is labeled in grams to allow the reader to get a picture of the magnitudes involved.
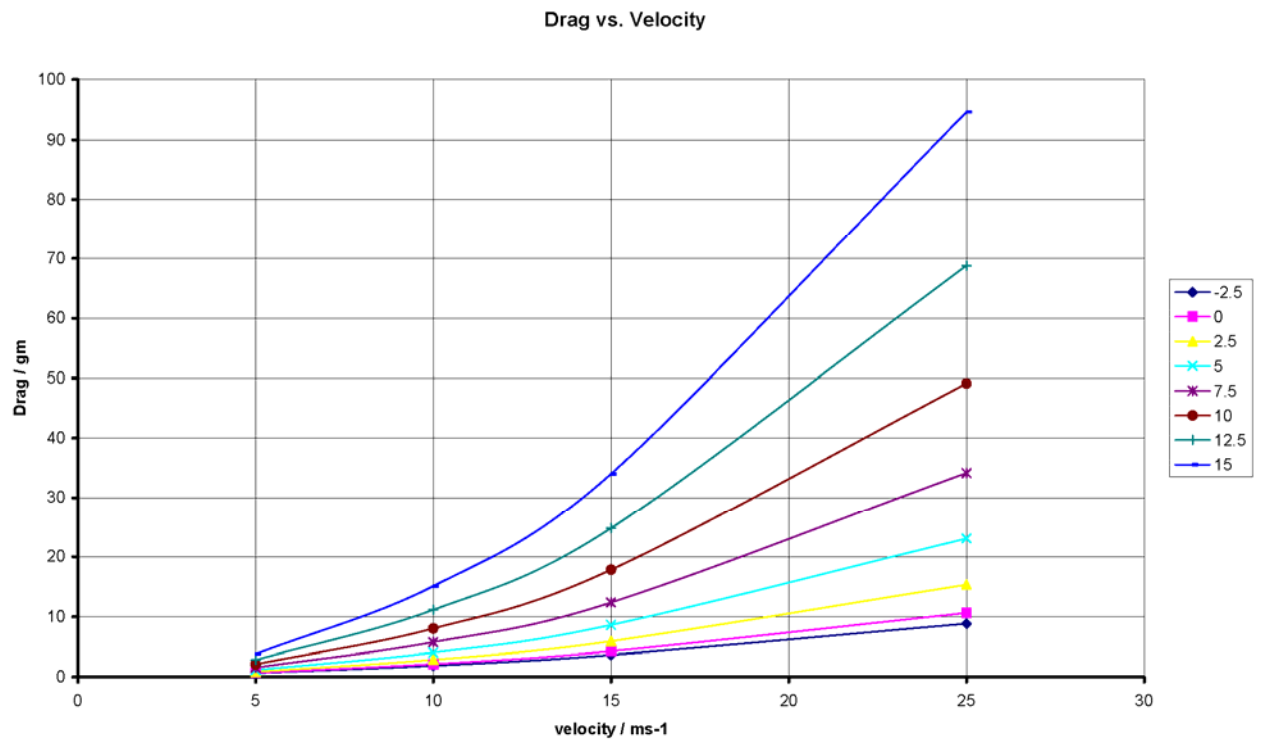
Figure 4.22 Drag variation with velocity

C F D

Further runs were done on the 20 m/s condition to find the stall angle of attack. This started at the 15 ^{o} angle of attack and runs were done at a 5 ^{o} interval. Stall occurred at approximately 28 ^{o}. It was more dominated with vortices produced at the tip than with simple separation.
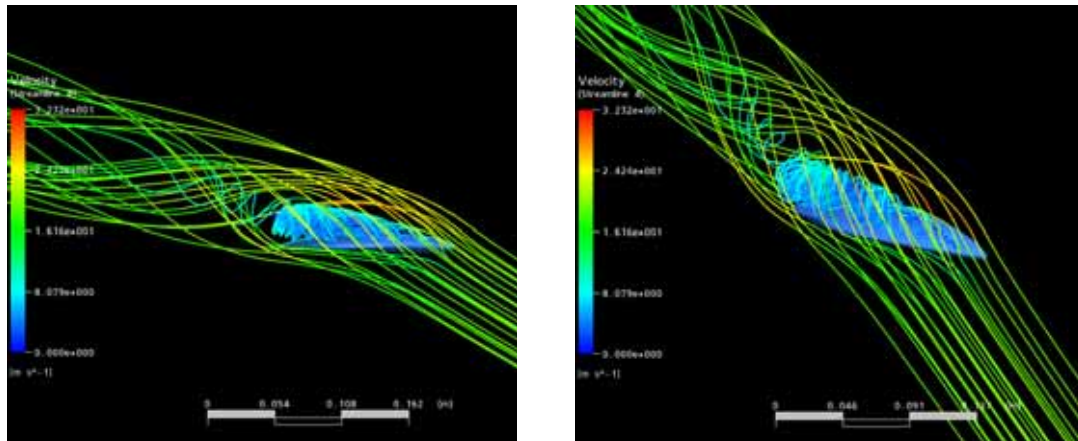
Figure 4.23 Stall streamlines for high alpha

4.5   Conclusion

The results overall showed that the MAV design would satisfy the requirements for the sustained flight and also showed optimistic endurance performance parameters.

The test results were compared with the wind tunnel test data shown in chapter 2 (figure 4.24). The data conformed quite accurately at low angles of attack up to 25 degrees, after which the computational model predicted a stall; where as the experiment showed a much later stall around 35 degrees for an inverse Zimmerman plan form.

Important to note though, the experimental data was collected using thin sections,
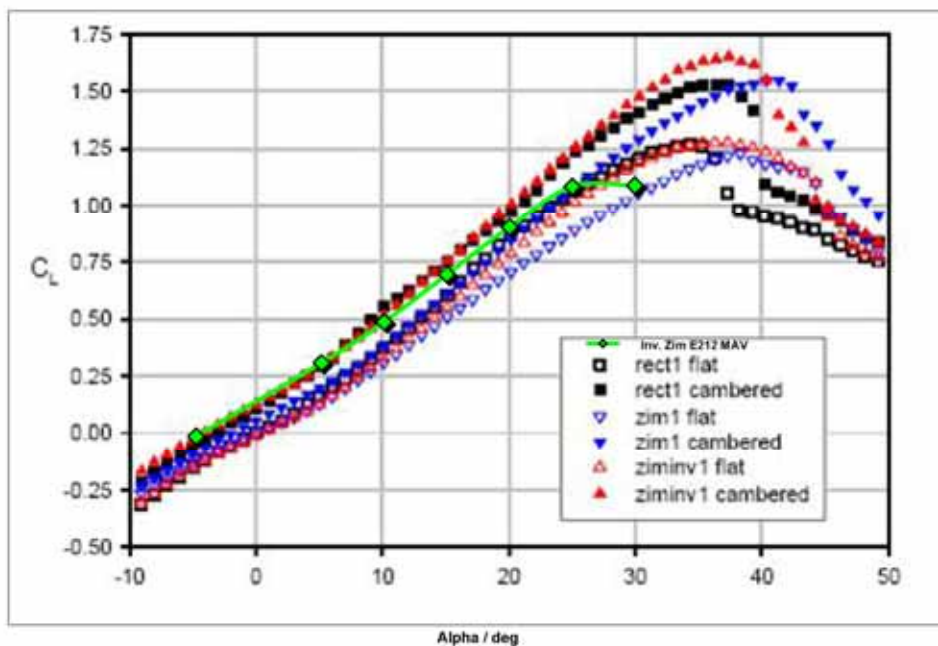
Figure 4.24 Comparison with experimental test data (computational data green line)

a flat plate and a cambered plate. This could be one source of the difference in stall prediction.

Another potential source for the discrepancy could be the turbulence model used for the computational solution. As mentioned earlier, we used a 4 equation model, and the incident flow always had 5% turbulence.

Moving on, given that the main criteria for MAV design were to maximize flight time, the angle of attack would be selected according to the maximum value of the Cl3/2/Cd curve at the chosen design speed.

In interesting issue revealed itself during the result analysis, concerning drag variation with the velocity. It was expected that at a certain velocity, a minimum value

of drag would occur, which would therefore produce a minimum value for the power required.

The results however, did not have a minimum value and seemed to continually decrease with decreasing velocity.

This therefore, dictated that we select a velocity based on the minimum lift required and maximum thrust available.

5   CHAPTER FIVE: STABILITY ANALYSIS

5.1   *Introduction*

The prospect of micro-scale flight, while enticing, presents a formidable set of challenges, of which the stability problem is a most serious one.

To be able to install a camera or indeed any kind of apparatus on the vehicle, to carry out the required mission, dictates that the aircraft be a stable flying platform, able to collect information with some degree of smoothness.

While considering our specific case, we concerned ourselves with longitudinal stability, as no data owing to lateral stability was produced during our research and computational analysis. We would compensate for lateral problems during the testing phase by adjusting vertical fin sizes and locations.

5.2   *Longitudinal stability*

In order to specify construction, our first step in the longitudinal analysis was to try and stabilize the wing using no more than elevator deflection. We went to add a horizontal tail when this approach failed. Finally we ran computational tests on the modified design to confirm stability.

5.2.1   Wing moment

From the computational analysis over the wing, we were able to locate the aerodynamic center and all associated aerodynamic coefficients.

Next we moved on to derive the center of gravity moment expression; which is as follows:

$$M_{cg} = M_{ac} + F_v (h_{cg} - h_{ac})$$

Where M_{cg} is the torque about the center of gravity, M_{ac} is the torque about the aerodynamic center and F_v is the vertical force.

From this expression we were able to calculate and plot the moment variation with the angle of attack, shown in figure 5.2. It was necessary after wards to relate the plats to the absolute angle of attack.

From the C_l-α curves we established the zero lift-line was at an angle of 4.2 degrees and hence the $C_{m\_cg\_w}$ was platted against the absolute angle of attack.

It becomes clear from the above plot that with the center of gravity ahead of the aerodynamic center the plane tends to pitch down at all positive angle of attack.

5.2.2 Elevons effect

A swift analysis of the effect of the elevons deflection then followed. We assumed the flaps to be rectangular and have a flat cross-section. We then calculated up to 40 degree using the aerodynamic data of a fate plate in chapter 2.

The elevon dimensions were set at the maximum had prescribed during the preliminary design.

The expression used:

$$M_{cg\_elevons} = -L_{ele}(h_{ac\_ele} - h)$$
$$L_{ele} = C_l \times S \times q_\infty$$

The results showed that at a maximum deflection the elevons could trim the aircraft at the angle of attack chosen at the end of chapter 4 which also meant that elevons were basically ineffective.

5.2.3 Adding Horizontal tail

To address the problem raised during wing analysis it became clear that a horizontal tail was needed.

It is important to note, however that the elevon analysis conduct involved a lot of simplification and can therefore be considered fairly inaccurate. For this reason we would still attempt to fly a prototype with no horizontal stabilizer to test stability experimentally.

5.2.3.1 Tail design

In order to simplify the tail manufacture, we designed the tail as a flat rectangular plate. Because we required only a moderate moment contribution of it, this was a fair trade-off in terms of overall efficiency.

Once again we would rely on the LAR data in chapter 2 to compute the tail contribution. From the first inspection of the data, it was evident that rectangular plates with AR 2 were the most efficient.

5.2.3.2 Tail contribution to pitching moment

The tail contribution to the moment in general is:

$$M_{cg\_t} = -L_t[L_t(COS(\alpha_{wb} - \varepsilon) + D_t SIN(\alpha_{wb} - \varepsilon) + Z_t L_t SIN(\alpha_w - \varepsilon) - Z_t D_t COS(\alpha_{wb} - \varepsilon) + M_{ac\_t}$$

To simplify this equation we neglect the down wash effect ε. Given the scale and simple cross-section of the tail, we saw it reasonable to also neglect the effect of the tail moment $M_{ac.}$

The tail moment contribution then became:

$$C_{m\_cg\_t} = \frac{-L_t S_t}{SC}[C_{l\_t}COS\alpha_{wb} + C_{dt}SIN\alpha_{wb}] + \frac{Z_t S_t}{SC}[C_{l\_t}SIN\alpha_{wb} - C_{dt}COS\alpha_{wb}] +$$

$$+ \frac{Z_t S_t}{SC}[C_{l\_t}SIN\alpha_{wb} - C_{dt}COS\alpha_{wb}]$$

This gave a tail moment coefficient as:

$C_{m\_cg}=C_{m\_cg\_wb}+C_{m\_cg\_t}$

5.2.3.3 Tail parameters

As mentioned before, the basic design required for MAV is to have no single dimension greater then 6''. This restricted the tail arm we could extend, which meant that the tail would be literarily immersed in the vortex wake from the wing.

To nullify this problem as much as possible we decided to raise the tail above the wing enough to minimize the downwash immersion from the stream lines calculated in chapter 4. The tail needed to be at 5 cm at least from the wing to receive clean air up to 15 degrees angle of attack.

Having set the first parameter, we went on to vary the rest in spreadsheet application and monitor the changes in the pitching moment curve.

- Note:

The addition of the tail shifted the overall aerodynamic center (neutral point considerably aft. This translated to more freedom for the center of gravity. In response to this, we shifted the design CG backwards to 7 cm to keep the static margin down.

5.2.3.4 Final tail parameters

	Tail config1	*Tail config2*
Tail location	17 cm	14 cm
Tail chord	5 cm	4 cm
Tail span	10 cm	8 cm
Tail Z	6 cm	5 cm
Tail installed angle	8^0	5^0
Aircraft CG	7.6 cm	6.5 cm
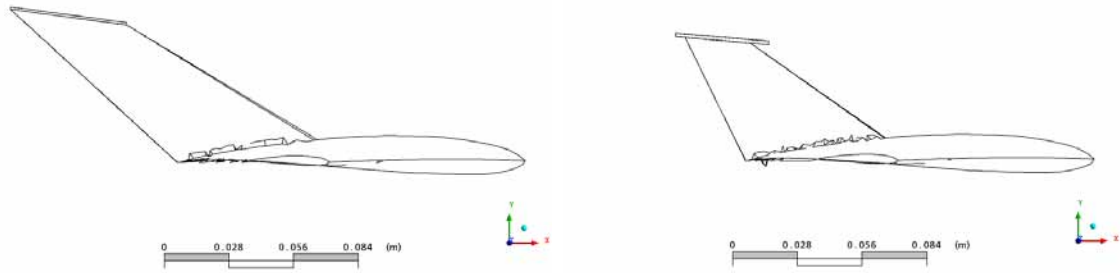
Figure 5.1 Tail config1 and 2

5.2.4 Computational tests

To confirm the tail analysis performed a set of trial computational runs we carried out on the new aircraft design. The results were as follows:
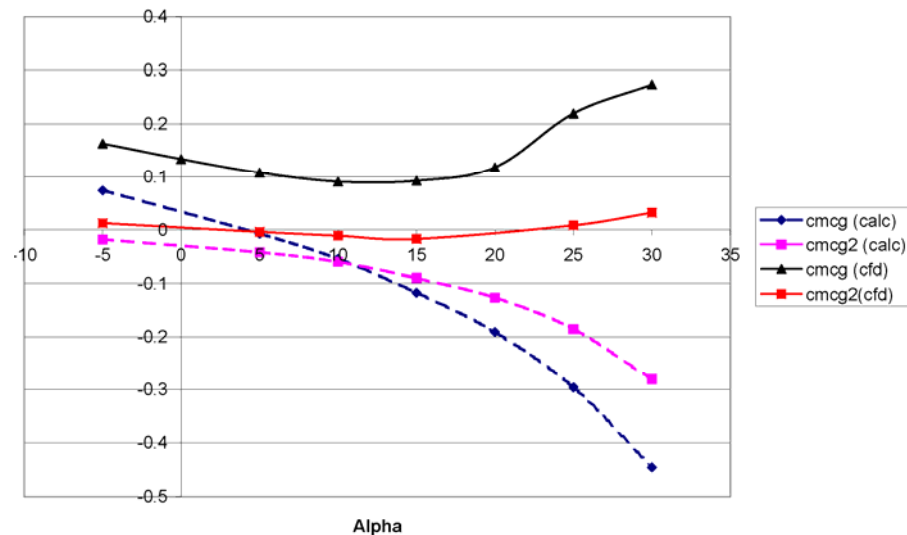
Figure 5.2 Comparison between pitching moment variation calculated using flat plate data and computational analysis

It can be seen above that the results calculated computationally do not conform at all to those initially determined using approximations. These approximations, however, aided in producing parameters for computational testing. Our earlier analysis of the numerical solution showed it to conform to the experimental solutions in moderate angles of attack; therefore we chose to rely on the numerical solution to select the tail unit.

We would go forward with tail configuration 2, as it trimmed at an acceptable angle of attack, and while the rate of pitching moment change can be said to be

extremely slow, we deemed it acceptable, and would modify this by moving the center of gravity further towards the leading edge.

5.2.5 Control

The issues of longitudinal control and control quantities were left to experimental analysis during flight testing.

5.3 Lateral stability

This phase of analysis was not fully carried out given that the mission did not require maneuvering or lateral stability (no camera). This approach was further emphasized by the lack of any technical and scientific research to refer to this flight regime.

We began the analysis by inspecting the flight characteristics of birds which used no vertical fins and relied on balancing during cruising flight.

This led us to the conclusion that should we be able to properly balance the aircraft laterally, we needed no vertical stabilizing provided we do not attempt rolling maneuvers.

This, however, was very optimistic design and therefore we referred to other MAN designs flown by design groups in order to design a vertical fin to act as a back up.

To conclude, our work on stabilizing the aircraft laterally, while overall was dodgy, would be further advanced during flight testing.

6 CHAPTER SIX: CONSTRUCTION

6.1 Introduction

This chapter is to focus on contracture steps and techniques followed in constructing the MAV of this project. Several ideas came out regarding the material of construction, tools used in construction, surface finishing, making a prototype model, and issues on construction concerning stability. Through this chapter reader will find what he would like to know about the construction process.

6.2 System Components

The electronic components used on the endurance MAV are required to be light weight, low power, and small in size. These components become the limiting factor in the size of the MAVs. A valuable source on the latest developments in micro R/C technology is http://www.bphobbies.com. This web site has been used as a source for many of the components. These components are listed in Table 1.

COMPONENT		WEIGHT
Battery Pack	Apache Lithium Polymer 3.7V 300mAh	2×8
Speed controller	Microbatics BLC-1 Single Cell Brushless Motor Controller (BLC-1)	0.5
Motor	Microbatics M5-30-60 High Performance Single Cell Brushless Motor (M5-3-60)	5.8
Propeller	(5 x 3) Direct Drive **Black** Electric Propeller (EP-5030)	1.4
Servo	Blue Arrow BA-TS-2.5 Micro Servo with White Micro JST Connector (White-Black-Red)	2.5
Receiver	Microbatics 4 Channel DSP Narrowband Receiver for Servos (DSP-S3)	2
Receiver Crystal	72 MHZ channel 11 Blue arrow receiver crystal	N/A
Total		**28.2**

Table 2: Components

1.6Figure

6.3   Components specifications

6.3.1   Battery

Weight:	**8.0 grams / .28 oz**
Capacity:	300 mAh
Voltage:	3.7V
Dimensions:	48.8 x 22.3 x 4.5 mm / 1.92 x 0.88 x 0.18 in.
Connector Type	Solder Tabs

6.3.2 Motor

Motor statistics are measured at 3.5 volts giving a modest measurement against the typical 3.7V single cell voltage. Motor is designed specifically for the GWS 5 x 3 propeller, and generates 60 grams of thrust at 3.5V while drawing 2.29 amps.

Features:

- Weight: 5.8 grams, 7.2 grams with GWS 5 x 3 propeller

- 14.1 mm (.56 in.) Diameter, 28.4mm (1.1 in.) Length (including shaft and tube mount)

- 1.5mm (.059 in.) Output Shaft

- Includes prop adapter for GWS 5 x 3 propeller

- Wires terminated with 3-pin 2mm connector for plug and play operation with BLC-1 ESC

- 14 magnet poles, 12 stator teeth

- 5.4mm OD / 3.6 mm ID aluminum tube mount

6.3.3 Receiver

Model:	DSP-*S3*
Operating Voltage:	2.9V - 4.2V
Receiver Weight:	2 grams
Weight with Antenna and Crystal:	2.7 grams
Antenna Length:	8 inches
Size:	21.3 x 11.2 x 7.3 mm
Outputs:	3 White JST Servo Outputs 1 Microbatics Stackable Port
Battery Connector:	Polarized EC-3 2mm Connector (Pin-Positive)
ESC:	n/a - Use BLC-1 or CM-1

6.3.4 Receiver crystal

Frequency tolerance is ±10ppm, pin is f0.35, operation temperature range from -20 to+70C and it's aging is ±5ppm/year.

- FM 72MHz Band

- Leg Diameter: 0.012 in.

- Leg Length: 0.25 in.

6.3.5 Speed controller

Brushless speed control designed for single li-poly cell use (2.9V - 4.2V). It weighs a mere 0.5 grams and measures an extremely tiny 0.31 x 0.42 in, yet can handle a whopping 3 amp draw with 10 second bursts up to 3.5 amps. Used with any single-cell standard servo-output receiver with a suitable servo adapter. The maximum commutation rate is 130,000 CPM which sets the maximum RPM to 18,000 for a 14 pole motor, 21,600 for a 12 pole motor, or 65,000 RPM for a 4 pole motor.

6.3.6 Servo

Dimensions (mm):	**19.6 x 16.2 x 8 mm / 0.8 x 0.64 x 0.3 in.**
Weight:	2.5 grams / 0.088 oz
Weight w/ Servo Wire:	2.8 grams / 0.098 oz
Ball Bearings:	No
Metal Gears:	No
Torque (4.8V):	2.08 oz.in.
Transit Time (4.8V):	0.12 sec./60°
Torque (6.0V):	2.36 oz. in.
Transit Time (6.0V):	n/a
Operating Angle:	40°/one side pulse traveling 400usec
Direction:	clock wise/pulse traveling 1500 to 1900usec
Static/Operating Current:	1mA - static / 100mA - operating
Dead Band Drain:	10uses
Connector Wire Length:	50mm

Construction

6.3.7 Propeller

Size (mm)	***127 x 76***
Prop Shaft Diameter (mm)	4.0
Weight:	1.4 grams

6.4 Designing MAV Wing

After CFD tests were made on several wing plan forms and airfoils decision was made on "Inverse Zimmerman" plan form and Epller212 airfoil. A model was drawn for the wing using UG (Uni-Graphics program). The Model shape is shown in figure 1.
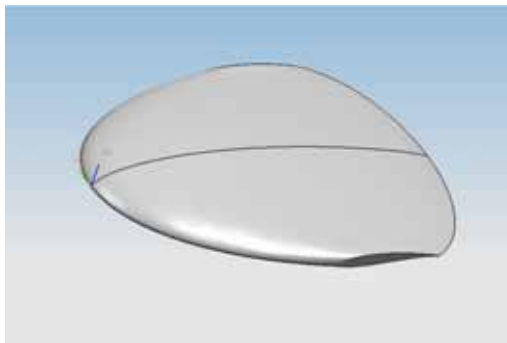
Figure 6.2 Full wing model
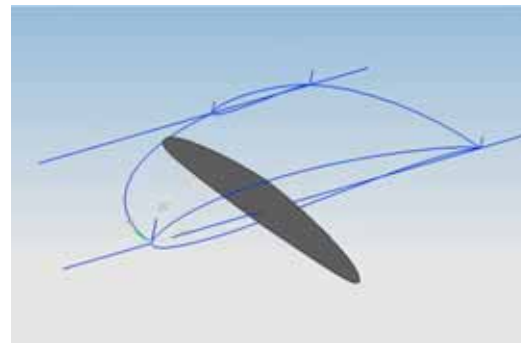
Figure 6.3 Section in wing model

Dimensions taken for the wing are as shown in figure 2 (dimensions are in inches).
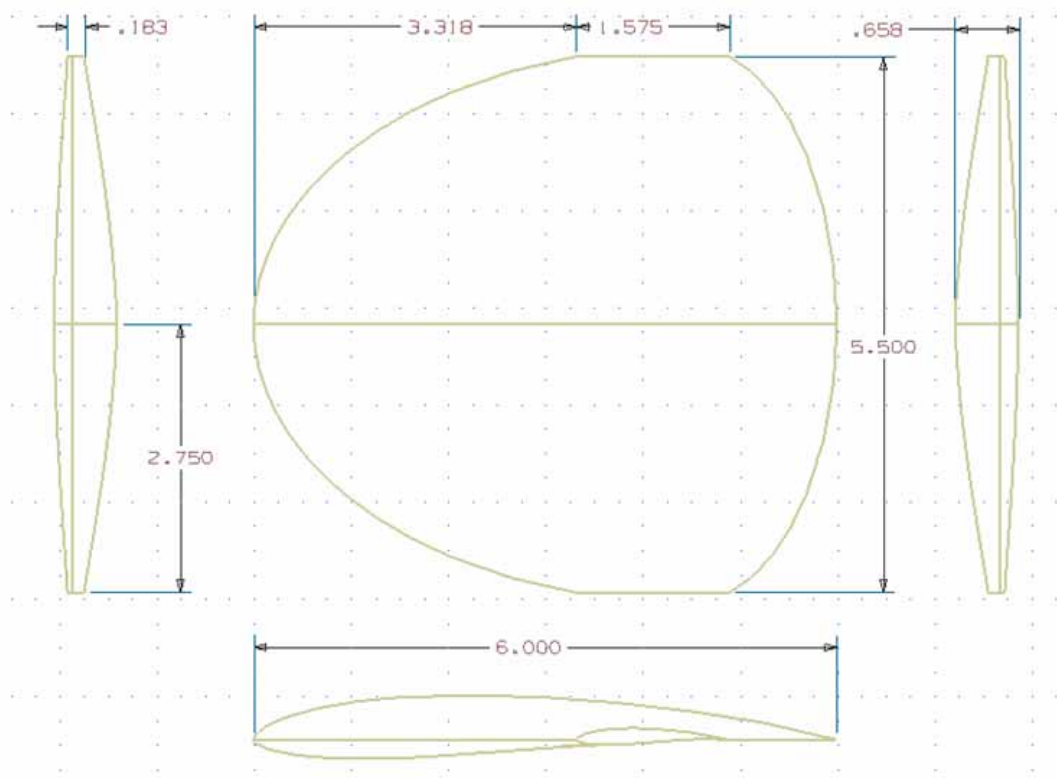
Figure 6.4 Wing Dimensions

As seen in the above figures a small cut on each of the wing sides is made to ease the manufacturing process of the wing.

6.5 Building MAV Wing

After designing the MAV wing ideas where set to construct and build an actual 3D model for the wing. At first a skeleton model was desired to have an idea how about how this model can be constructed. So, a 3D structure skeleton was made from balsa wood. Sections of the UG model was printed at different stages to build up ribs and flanges on plan paper then cut with a cutter. Cut sections were glued to a balsa weed sheet of 2mm thickness then cut with a cutter to for rips and flanges of balsa wood each of 2 mm thickness. Ribs and flanges are fixed together after that through slots grooved through each at certain places. A first prototype of that model was built and failed due to lack of experience in using balsa wood as row material then a second prototype was built and succeeded to give a pretty good idea about an actual 3D model of the MAV. Following figures shows the first and second 3D balsa skeleton model construction process.

6.5.1 First model:

1. Balsa sheet was fixed and got prepared for cutting process
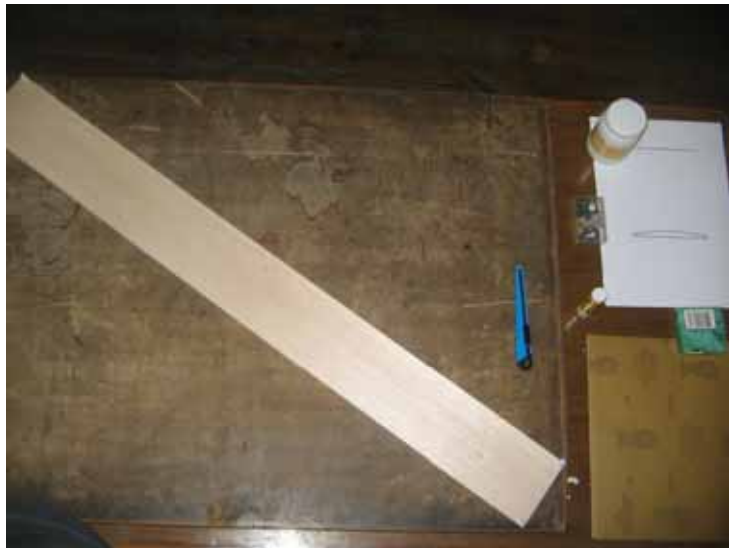
2. Printed sections are placed to be cut.

3. Printed sections are placed to be cut.

4. Balsa section are then grinded using sand papers to smoothen its edges

5. Sections are then grooved to prepared it to be fixed together
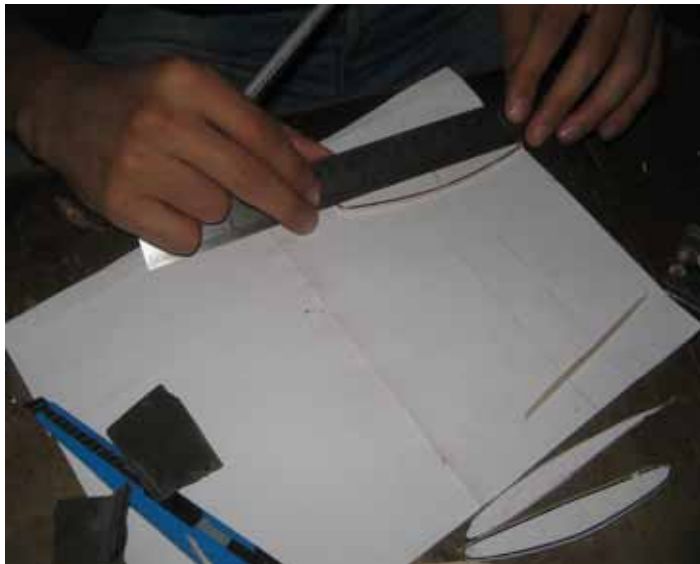
6. Then first model is fixed together

6.5.2 Second model

The second model building process was pretty much as the first one except that sections were more and experience was some how better. Follows figures show the process:

Figure 6.5 Second model sections cutting

Figure 6.6 Second model coating
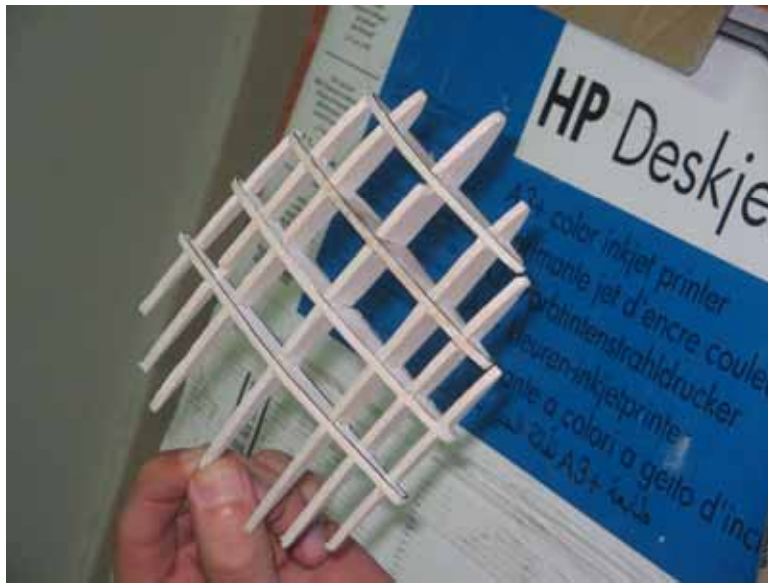
Figure 6.7 Second model finished

6.5.3   Third model

After constructing the balsa wood and having an idea of how the 3D model would look like there was a need to build a full 3D model (not just a skeleton) to use for building fiber glass body for the wing. Building the full 3D model was a challenge. The team had different ideas like constructing the model using CNC machine but it was too expensive. Then the team got an idea of cutting the whole model to sections each of 1mm thickness and then assembling all these sections together. That was a reasonable idea.

The whole section was cut to sections of 1mm thickness on UG then transferred to AutoCAD file so it can be cut on a 2D CNC laser machine (the machine can't read but CAD files). Figure below shows the file having half of the wing's sections (70 sections).

Construction

A 1mm thickness acrylic plastic was bought and section drawn on AutoCAD was cut on it.

Figure 6.8 Third model sections cut

Figure 6.9One of the sections of the third model

The 140 sections had grooves to guide the sections by a jig which goes through the grooves.

Problems appeared because the slots (grooves) were too small so manufacturing jigs for such slots was a hard task. Another problem faced the team when we tried to

assemble the sections together. It appeared that half of the wing had a width bigger than the other half. It appeared that the problem was that there was a defect in the acrylic plastic sheet that it wasn't uniformly of 1mm thickness. This problem was solved by exchanging sections positions between the two half (like taking no. 2 in the 1st half and changing it with no. 2 in the 2nd half then leaving no. 3 and doing with no. 4 what we did with no. 2 and so on). Figure below shows the problem.

Figure 6.10 Sample of the model's two halves width variation

Figure 6.11 Same sample after solving the problem

6.5.4 Jigs manufacturing

As the wing was cut to 140 sections a jig was required for assembling those sections together. Two slots of 1.2mm thickness and 6mm wide were made along the wing width through all the section (as in figure). The challenge was to manufacture a stiff metallic ruler of 1.2 mm thick and 6mm wide because metal cutters at the workshop couldn't cut that small width in such small thickness of metal. The team found that stainless steal in such thickness and very small width can't give the needed jigs as it deforms (as shown in fig 8). So, carbon steal was used instead. After some trials the jigs were cut then grinded.

Figure 6.12 Failed trials of jigs making
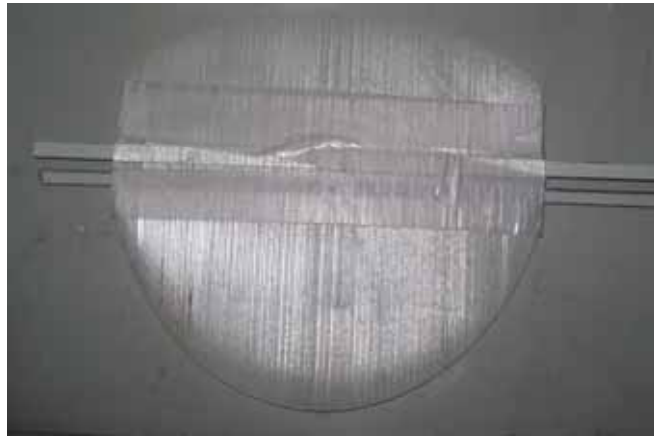
Figure 6.13 Full wing after asembly using the final jigs

6.5.5 Model Assembly

After finishing the cutting and jigs the assembly process took over. Acrylic plastic is bonded together by a substance called chloroform. The interesting part about that adhesive liquid is that in melts the acrylic and bond it together like if is a welding process. This means that there is no extra thickness after the assembly of the wing.

Painting brushes were used to run chloroform over the wing and after few seconds the wing is assembled.

Figure 6.14 Model sections fixing

Figure 6.15Wing model after fixing

6.6 Fiber Glass Body

The leading edge was actually the part which was planed to be made of fiber glass due to weight considerations. A fiber glass leading edge was needed because of the complexity of manufacturing a leading edge a Zimmerman plan form and a leading edge of an Eppler 212 airfoil.

A first trail was made and shown in figure below:

Figure 6.16 First trial of fiber glass leading edge

However, this leading edge was not used for weight considerations (as previously mentioned), lack of time problem facing the team, and lack of experience and equipments. It was left for another research phase.

6.7   First Prototype

A 3D design was made on UG for
a full prototype made of balsa wood
with all the components installed in
it.
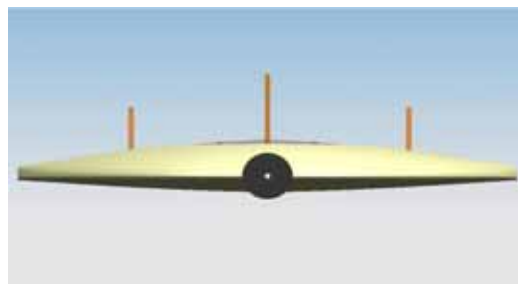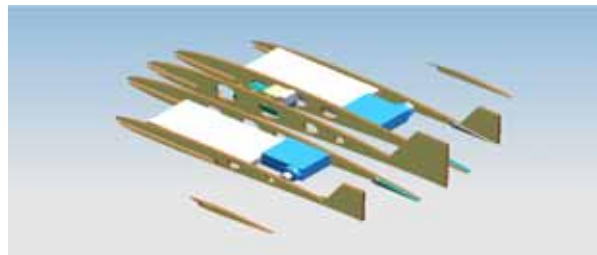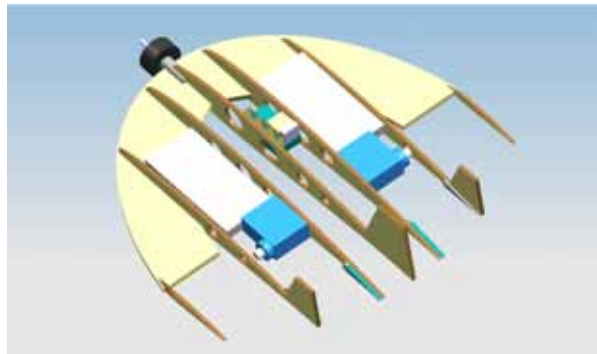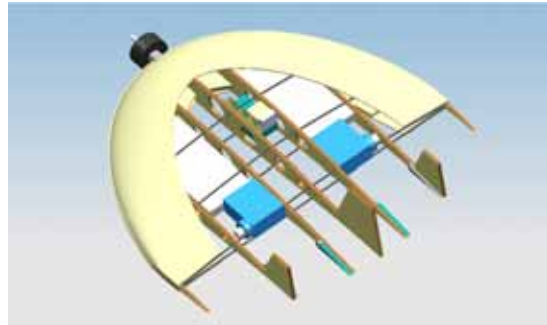
The first prototype was built from balsa wood. With the same technique used to cut the acrylic sections, balsa sections were cut except of course that it was less sections; 5 flanges and a 2D leading edge. Flanges were glued to the 2D leading edge.

Figure 6.17 Negative cut of first prototype

6.8 Second Prototype

A second prototype was built because the first one did not have the camber of the Eppler airfoil because of he relative wide spaces between flanges.

In this second prototype some spurs were added to give the camper of the airfoil.

Flanges were glued with the 2D leading edge and the spurs. Fate control surfaces were made.

Components were prepared to be installed in the prototype

84

Control surfaces were hinged to the prototype

85

Components were installed.

6.9 Third Prototype

The second prototype had some technical mistakes; cuts for the battery charging wire were made on the upper surface and also the rods connecting the servos with the control surfaces were also made on the upper surface. Also the vertical tail connection wasn't installed. So a third prototype had to be built to correct these mistakes.
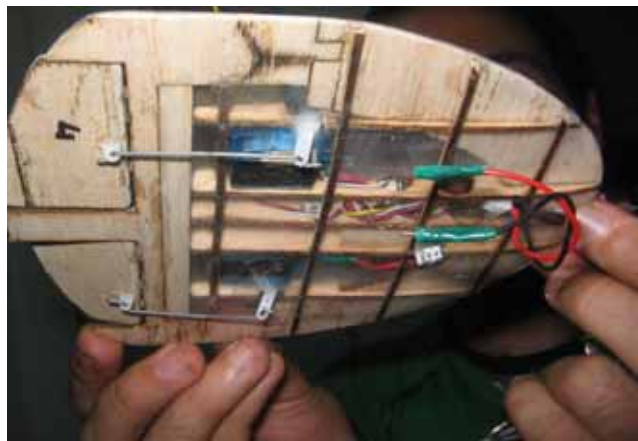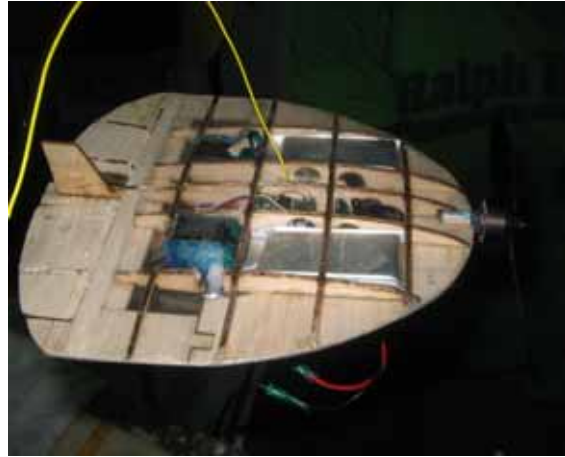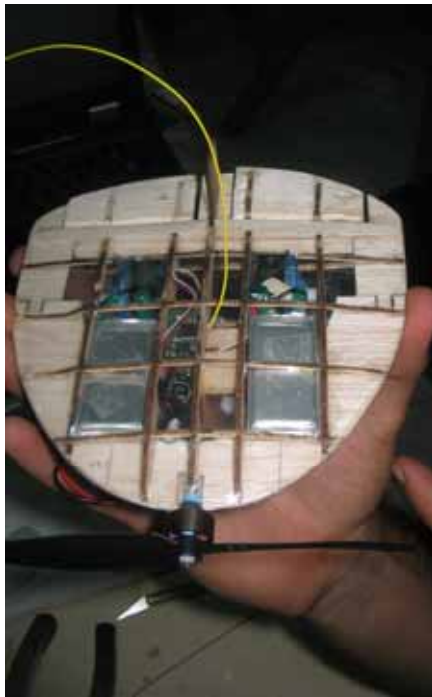
7 CHAPTER SEVEN: RESULTS

7.1 Introduction

Having completed the construction phase, we moved on to the testing phase. We carried out a number of static tests on the components and the aircraft. In this chapter we outline the procedures, their outputs and the problems faced.

7.2 Initial prototypes testing

The first two prototypes were not extensively tested; they were weighed to get some indication of the structure mass range. Furthermore, the second prototype was tested in terms of components installation and connection. Due to the eight space available inside, the prototype was designed and cut with no explicit trailing edge parameters.

A final test conducted on this prototype was a battery connection test. We tried components using a high 7.4 voltage and standard 3.7. The tests were qualitative; to determine weather the 3.7 would be sufficient to operate the entire system with no drop. Results were positive.

7.3 Third prototype testing

The third prototype was created based on the initial findings and was used for actual performance tests. In addition, this prototype had a tail unit supplement designed and fabricated to be added and removed for stability tests.

7.3.1 First flight test:

To begin with, the purpose of this test was to attempt to fly the MAV without any stabilizing surface, relying on its own stability and user input on the control surface.

The test procedure was simply to turn on the system, test surface response and motor response before launch, secure battery and hand launch.

The success criteria for this test were to achieve sustained flight and maintain a relative heading. Failure tolerance was battery consumption and structural failures.

Suffice to say, this test produced somewhat disappointing results. The MAV was able to propel itself, however, once launched instability both laterally and longitudinally dominated and a swift crash followed.

A number of attempts were made to vary launch direction, angle of attack and control surface trim, these were to no avail, the intensity of instability did not leave any window for control.

Laterally, the MAV would instantly go into an uncontrollable roll, spinning through the air, no exact data was collected as the rate of events did not allow for human data collection.

Longitudinally, it was somewhat difficult to rate the exact pattern, largely due to the dominate roll. However, the general consensus from the testing team was that the

craft tended to pitch up at positive angles of attack, and pitch down at negative angles of attack. This was enough to register as instability.

7.3.2 Second flight test

Unfortunately, we were never able to conduct a second flight test. This was on account of the transmitter compatible with the MAV receiver became unavailable, and despite our best efforts we were unable to supply another one.

7.3.3 Static testing

The only static test planned was a test of thrust force variation against throttle lever position.

To carry out the test we used a sensitive balance, a smooth roller and a set of weights. The procedure was as follows:

1. the weights were put on the balance after it was calibrated

2. the roller was set up to be in a position directly over the weights

3. a light wire was connected to both the aircraft and the weights, at its ends

4. the wire was passed over the roller, this allowed the thrust force (horizontal) to act as a vertical force on the weights

5. the aircraft was secured in such a way so as to only allow movement in the X-direction

6. the system was checked for smoothness by moving the aircraft forward

7. the motor was started and then set at the zero position reading was noted

8. we varied the lever position at set intervals and collected thrust data

   Thrust = (Throttle off weight) – (position N weight)

Once again, due to the unavailability of a compatible transmitter, no results for the static test were produced. The test procedure was, however, set up and checked as mentioned above, in the case the communications issue was resolved at any point.

8 CHAPTER 8: CONCLUSION

Originally the goals set for this project were to produce an endurance MAV able to maintain a heading and sustain flight for as long as possible.

8.1 Stability issues

The first flight test brought to attention a number of stability problems, as described in chapter 7.

8.1.1 Lateral stability problems

The MAV showcased appalling lateral stability during the test. We attributed this to two main design shortcomings. Firstly, the absence of a vertical stabilizer. This was to be addressed in the second test. Sadly, we cannot verify the effectiveness of this modification on account of the second test not taking place.

The second source of this instability was the poor span wise distribution of the masses. This led to a low mass moment of inertia about the X-axis. Since the components were mostly installed within 1'' of the root chord, the engine torque acted heavily on the aircraft producing a large roll rate. Addressing this problem is somewhat more complicated, due to the limited space available inside the MAV, spreading the mass distribution requires compromises to the aerodynamics to allow for geometry changes. Another solution would be to fabricate custom components; however this was beyond the scope of this research.

8.1.2 Longitudinal stability problems

This problem proved a lot easier to resolve; the addition of a horizontal tail corrected the problem. However, this came at the expense of the total lifting force, and the increase in drag.

After this issue first became evident, we went back to the computational analysis to attempt to investigate the source of the problem and address it with minimum losses in performance. We concluded then that the modified Eppler with its reflexed trailing edge camber would possibly been better poised to address the issue of longitudinal stability.

8.2 Construction issues

8.2.1 Balsa wood

The conclusion we arrived at from working with balsa wood was as our main structural material was that its use was not practical beyond experimental and prototyping purposes.

To elaborate, while its extremely low density makes it light weight, the poor hardness and unidirectional strength severely reduce its durability and survivability. During testing, and even construction, the wood was too easily scratched and chipped.

8.2.2 Fiber glass and plastics

Our efforts to produce a fiber glass reinforced body were mainly driven at creating a more standardized production process as well as increase survivability, especially during testing.

The lack of expertise slowed our progress in the fabrication. Furthermore, the small size of the MAV and the level of detail involved complicated mold creation. Towards the end of our work in this field we were developing a mold-less casting technique. We had to terminate development, however, due to time constraints.

It was our conclusion that producing a fiber class reinforced body, or even better a carbon fiber reinforced body was realizable. However, it required more time and attention we became a constraint towards the end of our MAV development.

8.3 Final consensus

It becomes clear at this point; that should the stability issues be eliminated or at least scaled down, the endurance goal would be easily satisfied. However, it also becomes clear that the order of this endurance would be of minutes rather than hours. This is mainly a result of the technology limitations of battery storage.

Future development of this MAV should include optimizing the airfoil used, decreasing overall size and weight, experimenting with other propulsion systems (MEMS turbines, micro pulse-jets, etc…) and adding an autopilot system to smooth out the dynamics and allow inexperienced user operation.

A References

[1]   Grasmeyer, J.M. and Keennon, M.T., "Development of the Black widow Micro air Vehicle" AIAA paper No. 2001-0127 2001

[2]   Wei Shyy and Peter G. Ifju, " Flexible-Wing-Based Air Vehicles" AIAA paper No. 2002-0705

[3]   Mark Derla, "Higher-Order Boundary Layer Formulation and Application to Low Reynolds Number Flows" AIAA paper

[4]   Peter J. Kunz and Itan Kroo, Analysis and Design of Airfoils for Use O\at Ultra-Low Reynolds Numbers" AIAA paper

[5]   E.V. Laiton, "Wind Tunnel Tests of Wings and rings at Low Reynolds Number", AIAA paper

[6]   Torres, G.E. and Mueller, T.J., "Aerodynamic Characteristics of Low Aspect Ratio Wings at Low Reynolds Numbers", AIAA paper

[7]   ANSYS ICEM and CFX V10.0

[8]   UniGraphics V4.0

[9]   Dr. Peter Ifju, "Design of the University of Florida Surveillance and Endurance Micro air Vehicle, University of Florida, FL 32611-6250

[10]   P. Geuzaine, "Flow Simulation Around a Micro Air Vehicle in a plume Characterization Scenario" University of Colorado, 80309-4429

[11]   Gabriel E. Torres, "Aerodynamics of Low Aspect Ratio Wings at Low Reynolds Numbers with Applications to Micro Air Vehicle Design" University Of Notre Dame.

[12]   James Brit Whistle, "An Investigation into Micro Air Vehicles", Lough Borough University.

References

[13]   David A. Jenkins, Peter G. Ifju and Mujahid Abdurahim, "Assessment of Construability of Micro Air Vehicles"

[14]   Scott M. Ettinger, "Design and Implementation of Autonomous Vision-Guided Micro Air Vehicle" University Of Florida team "University Of Florida competition Micro Air Vehicle" University Of Florida, FL 32611-6250

[15]   John D. Anderson Jr., "Introduction to Flight", McGraw-Hill, Forth Edition

[16]   John D. Anderson Jr. "Aircraft Performance and Design" McGraw-Hill, First edition

B Project Budget

Description	Value
Components for MAV	3,240.00
Balsa wood 1.5mm and misc. tools	12.00
Acrylic glass sheet 1mm	174.00
Laser cutting trial 1	148.00
Laser cutting trial 2	140.00
Plastic model and chrome steel leading edge	370.00
Laser cutting trial 3	140.00
Balsa sheet 1.5 mm	17.00
Laser cutting balsa	10.00
Technician first payment	150.00
Balsa	25.00
Electrical tools and wires	20.00
Workshop tip	5.00
Laser cutting trial 4	5.00
Balsa sheet 1.5 mm	8.00
Laser cutting trail 5	40.00
Balsa sheet 1.5 mm	18.00
Laser cutting trail 5	73.00
Balsa sheet 5 mm	9.00
Balsa sheet 1.5 mm	19.00
Technician second payment	200.00
Total	4,823.00

C Correspondences

MAV 2007 team had cooperation and assistance from a PhD Candidate in University of Florida. MAV 2007 team wanted to thank Mr. Mujahid Abdulrahim for his valuable help. Mr. Abdulrahim had his graduation project and his master thesis in MAV research field. He has many papers that he either published or participated in its publishing. For contact with Mr. Abdulrahim: **mujahid@ufl.edu**.

Correspondences with Mr. Abdulrahim are published in this appendix.

A.1 EMAIL #1:

Dear Sir, Mujahid Abdulrahim,

Al salam alikom wa rahmoto Allah. I hope this emails finds you in best conditions!

First allow me to introduce myself. My name is Abd El-Rahman El-Saied. I'm an Egyptian student at Cairo University, Faculty Of Engineering, Aerospace Department (sorry for the long term but that's how they write it!). I'm in fourth year (which is the graduation year). In my final year I've a graduation project (I guess that's how it goes in every engineering college). I was surfing the web in the past 5 month for a good topic for my graduation project. I found the page of "Journal of Undergraduate Research" at University of Florida which was about your graduation project; I found it in my early web research work. I was really amazed by the project and kept searching about it and about your work. I also found your Master degree thesis and some other papers you've published and I want to let you know that I really admired you work, Sir!

I decided to take your foot steps and try building a MAV as my graduation project. I talked to an Aerodynamic professor (Dr. Basman El Hadidi) about the idea and I found that he was more interested about it than really was and he accepted to supervise my MAV project.

However we have a very big problem, Sir, and I'm in real dispirit need for your help. The problem is that we don't have any equipments or laps in the department. As a matter of fact we have laps but it is very very old (from the 60's) and it is not even working now because the university isn't putting any budget for the department since 1967 war and the department even closed twice in it's life time. No money for equipments and laps means no money for research also. I'm very ashamed to say that almost (if not the entire system) all our study is theoretical and passed on texts and lecture notes which are (logically) too old (60's) except for some new blood that gives some life to the department as the department's PHD degree holders come from outside and try to show us the new things they have seen outside Egypt (mainly the US) (like Dr. Basman) [The staff of the department can't have their PHD in the university because of the lack of equipments, so they have to go outside and have their PHD and return back].

I'm sorry to waste your time with this long story that might mean nothing to you, but the problem I need help for is that I can't build or have by any mean a DAS (Data Acquisition System). I really hesitated so much to annoy you by this but I had no choice but to ask for your help. I need the data you had from the DAS and maybe some ideas about how did u manage the project and it's

ideas. I'd use your DAS in some optimization and CFD calculations and this might add something to your project.

I'd ask for more, hoping that u would allow me to relay on your generosity and kindness; I'd ask for your supervision on my project (As a distance supervisor). I hope I'm not asking too much and hope I'm not annoying you, Sir!

Happy Ramadan to you, Sir! (Kol aam we enta bekheer we sehha!)

Waiting for your reply

Yours

A. El-Saied

A.2   EMAIL #2:

Shukran kteer 3ala emailak. Insha' Allah kul 3aam wa anta bikhair wa rabbina yatqabal ta3atak.

Mabrook on getting close to graduation at your university. I hope that you both enjoy your studies and have a good final project. I am happy to help in any way that I can, although I have some limitations in resources.

I am not quite sure what you intend on pursuing for your project apart from involving a data acquisition system. Are you interested primarily in a wind-tunnel, static loads, flight test, or otherwise? The infrastructure needed to undertake any serious research is substantial, but you can probably design a low-cost experiment if you can clearly identify a problem you wish to solve/study. Depending upon your project, you can try to leverage whatever equipment you have or can get by donations and still perform a decent experiment.

The DAS systems have caused me great strife and disappointment over the years. The small devices you saw in the JUR paper were made by a company on contract with NASA for a bit over $100K. They stopped producing them and refuse to support them, so eventually all of our working models were destroyed in flight test incidents. We have recently been using the "Flight Data Recorder" from greatnorthernmodels.com. It has a fraction of the capability of the other DAS, but it is easily available and less expensive. The devices I use are owned by the university so I am not able to lend or donate them. I can offer mostly literature resources and help with technical issues, as you require.

If you are interested in embedded devices, you may also consider Gumstix (www.gumstix.org), which are small boards that have basic input-output capability along with a Linux 400MHz computing platform.

For flight projects, you can purchase a hobby remote control airplane (www.towerhobbies.com, www.aeromicro.com, www.hobby-lobby.com) and modify it for your experiment. For instance, you can study the effect of various flap or high-lift devices on the performance of the aircraft. You can also study controllability and handling qualities issues with different control surface configurations. If you cannot get a data acquisition system, you can plan your flights carefully (assuming you are able to pilot the vehicle) to measure simple performance data.

Finally, if you are doing a lab/bench project (as opposed to flight), you can use a computer-based data-acquisition board instead of spending a much larger sum on a micro DAS. If you are interested in this, I can suggest some relatively inexpensive boards to buy and interface with your computer.

Let me know how I can help.

Ma3a   alf   salamah,

Mujahid

A.3 EMAIL #3:

Dear Mr. Mujahid, I hope this email finds you in best conditions!

We (my project mates and me) were wondering about the temperature of the oven that you used to "bake" the carbon fibers of your MAV's wing!? And another 3 small extra question; how much time do you need to keep the wing in the oven!? Does the oven have to be vacuumed?! And if it's a special oven (vacuumed oven) why do I've to use a vacuum bag (is it a plastic bag or another material)!?

Thank you!

yours

Abd El-Rahman

A.4 EMAIL #4:

Salamz Abd El-Rahman, My apologies for not responding... I must not have seen your email. I get a lot of mail, so it may have been lost in my inbox. In any case, don't worry for a second about annoying me, quite the opposite. If I don't respond to your email, then try sending me another reminder, just in case I forgot about the first one.

I will look through my emails tonight, but what may have happened was I didn't respond while I thought about your request, then I ended up getting busy and neglecting to respond. But you may feel free to ask whatever you want - there's just no guarantee that I can provide. Insha' Allah I will do whatever I can to help out though.

Here are some answers to your questions:

1 - The curing temperature depends upon the type of resin used in the pre-impregnated or wet-layup carbon fiber. Whatever source you used to get the material should provide details on the cure cycle. We use either 260 deg F or 350 deg F depending on the type of carbon fiber.

2 - The cure cycle takes a total of 6 hours, where the first hour is a ramp from room temperature to cure temperature, the next four hours are constant at cure temperature, and the last hour ramps down to room temp. This can be shortened depending on the resin.

3 - The part does not have to be vacuumed, but doing so will give you far better results then leaving it open. The vacuum helps the resin bond to the fibers and can draw excess resin from the structure. It also gives a much nicer finish.

---

4 - The vacuum bag material is usually some sort of mylar that is specially made for composite layup. You will need to put breather cloth (cotton) and release film to allow proper suction distribution and prevent the vacuum bag from sticking to the part.

I hope this helps. Let me know if you have any questions.

Take care,

Mujahid

A.5 EMAIL #5:

Salamz and Eid Mubarak,

A. EL-S wrote:

Dear Mr. Mujahid, I hope you had had a happy Eid.

a. The amount of carbon fibers I might need to construct a wing with the dimensions you used for your endurance MAV wing and body.

The amount of carbon fiber is trivial, roughly 30cm x 10cm of carbon, depending upon your construction style.

b. Where can I buy "carbon fibers" in the USA? (We will ask some people we know who are returning to Egypt to buy them for us).

Do a search for aircraft carbon fiber on google to fine many resources. Here's one that is dependable. http://www.aircraftspruce.com/menus/cm/carbonfiber.html

c. How much does it cost!?

Check the sites, the price varies considerably.

d. What is the deference between the "pre-impregnated "and "wet-layup" carbon fiber?

I use pre-preg, which includes the resin/matrix in the fiber weave. To cure, you draw a vacuum and
place in the oven. The wet-layup requires you to manually apply the resin/epoxy to the fiber, which is more messy and challenging.
Ma3assalama,
Mujahid

I مـــــلخـص

هذا المشروع هو خطوة اولى في البحث حول المركبات الطائرة الدقيقة. المركبات الطائرة الدقيقة هي

طائرات متناهية الصغر تصمم لأغراض المراقبة الجوية دون الحاجة إلي قيادة بشرية مباشرة. هذه الطائرات

تصمم بحيث تكون قادرة على إتباع مسارات معينة بطرية آلية أو عن طريق التحكم عن بعد. مهمة مثل هذه

المركبات قد تكون عمل مسح قصير المدى أو للمراقبة أو إستشعار أي مواد خطرة. هذا البحث يتناول تصميم و

بناء نموذج لمثل هذه الطائرات من منظور تحقيق أقصى مدة طيران ممكنة. العديد من الأ بحاث التي تناقش

الدناميكا الهوائية للسرعات المنخفضة كانت قاعدة للبدء في عملية تصميم هذا المشروع و تم إنجاز المزيد من

التحليلات بالطرق الحسابية للتوصل إلى المزيد من البيانات التي ساهمت في إنجاز هذا المشروع. أيضا تم عمل

إختبارات لدراسة إتزان التصميم. و قد تم بناء عدد من النماذج الإختبارية لتوقيع الإختبارات العملية الإستاتيكية و

الديناميكية. و قد أثبتت النتائج ان إنتاج مثل هذه المركبات الصغيرة الحجم ممكن بل و إيضا عملي. إضافة إلى هذا

الأستنتاج كان من الواضح أنه توجد حاجة للمزيد من الأبحاث لإظهار مدى فاعلية و إمكانيات مثل هذه المركبات

لهذا السبب سيتم في مراحل لاحقة إدراج نظام قيادة آلي و كاميرات دقيقة الحجم مزودة بأجهزة بث متناهية

الصغر مع توفير الوزن قدر الإمكان لوضع معدات إستشعار و قياس أكثر تطورا.

CU-M.A.V. VER1.0

مشروع التخرج للعام الدراسي الرابع

أعداد

عبدالرحمن السعيد   طارق محمد البنّا   أكرم محمود عبدالصبور

إشراف

د. بسمان الحديدي